Copy
RM L52L24

NACA RM L52L24

NACA

RESEARCH MEMORANDUM

PRELIMINARY THEORETICAL INVESTIGATION OF SEVERAL METHODS FOR STABILIZING THE LATERAL MOTION OF A HIGH-SPEED FIGHTER AIRPLANE TOWED BY A SINGLE CABLE

By Albert A. Schy and Carroll H. Woodling

Langley Aeronautical Laboratory
Langley Field, Va.

NATIONAL ADVISORY COMMITTEE FOR AERONAUTICS

WASHINGTON

March 13, 1953

NATIONAL ADVISORY COMMITTEE FOR AERONAUTICS

RESEARCH MEMORANDUM

PRELIMINARY THEORETICAL INVESTIGATION OF SEVERAL METHODS FOR STABILIZING THE LATERAL MOTION OF A HIGH-SPEED FIGHTER AIRPLANE TOWED BY A SINGLE CABLE

By Albert A. Schy and Carroll H. Woodling

SUMMARY

A preliminary theoretical investigation of the lateral stability of a towed high-speed fighter airplane has been carried out. The analysis was conducted for a fighter cruising at supersonic speed at an altitude of 50,000 feet. For the basic towing configuration, a 1,000-foot cable was assumed to be attached to the nose of the fighter. Motions were calculated from lateral equations of motion which had been developed by other investigators on the assumption that the dynamics of the towing airplane and cable could be ignored.

The motion of the basic case is shown to have a highly unstable oscillation caused by the towline restraint. This preliminary investigation shows that the configuration may be stabilized both by choosing the right position for the towline connection and by several types of automatic controls. The automatic controls are assumed to have no lags.

Motions are calculated for various modifications of the basic case. Two methods of stabilization are presented which show promise of being practical. Both methods require automatic control. One type provides a side force and yawing moment proportional to sidewise velocity or sidewise acceleration or both; the other type provides a rolling moment proportional to angle of bank. Although the methods investigated herein for obtaining stability by adjustment of the towline parameters are shown to be impractical, the possibility of obtaining practical stability by adjustment of towline parameters is not dismissed.

INTRODUCTION

The possibility of a supersonic or transonic bomber's towing a high-speed fighter airplane has been suggested as a means of increasing

[redacted]

the range of the fighter. Previous investigations into the stability of towed gliders have shown, however, that lateral stability is difficult to obtain for towed aircraft (see refs. 1 and 2). The present paper is an exploratory theoretical investigation of possible methods for stabilizing the lateral motion of a fighter towed by a single towline.

The theoretical analysis of the stability of towed gliders presented in references 1 and 2 assumes that the disturbance of the motion of the towing airplane and the dynamic characteristics of the towing cable may be ignored. This assumption is also valid in the present case because of the small weight of the fighter relative to the towing bomber. The dynamics of the bomber and the towing cable should therefore be relatively unimportant if the lateral motion of neither the bomber nor the cable has a characteristic oscillation whose period is close to the period of a characteristic lateral oscillation of the towed fighter. Thus, in most cases the approximations used in references 1 and 2 are justifiable. Since these approximations greatly simplify the analysis, the equations of motion for a towed airplane which are derived in references 1 and 2 are used in this paper.

SYMBOLS

The forces and moments are referred to the stability axes. (See fig. 1.)

ϕ angle of bank, deg or radians

ψ angle of yaw, deg or radians

β angle of sideslip, deg or radians

δ deflection of control surface, deg or radians

γ angle of flight-path inclination, deg or radians

V airspeed, ft/sec

ρ mass density of air, slugs/cu ft

q dynamic pressure, $\frac{1}{2}\rho V^2$, lb/sq ft

b wing span, ft

S wing area, sq ft

W	weight of airplane, lb
m	mass of airplane, W/g, slugs
g	acceleration due to gravity, ft/sec^2
μ_b	relative-density factor, $m/\rho Sb$
α	angle of attack of reference axis with respect to flight path, deg or radians
ϵ	angle between reference axis and principal axis, positive when reference axis is above principal axis, deg or radians
η	inclination of principal longitudinal axis of airplane with respect to flight path, positive when principal axis is above flight path at the nose, $\alpha - \epsilon$, deg or radians
k_{X_0}	radius of gyration in roll about principal longitudinal axis, ft
k_{Z_0}	radius of gyration in yaw about principal vertical axis, ft
K_{X_0}	nondimensional radius of gyration in roll about principal longitudinal axis, k_{X_0}/b
K_{Z_0}	nondimensional radius of gyration in yaw about principal vertical axis, k_{Z_0}/b
K_X	nondimensional radius of gyration in roll about longitudinal stability axis, $\left(K_{X_0}{}^2\cos^2\eta + K_{Z_0}{}^2\sin^2\eta\right)^{1/2}$
K_Z	nondimensional radius of gyration in yaw about vertical stability axis, $\left(K_{Z_0}{}^2\cos^2\eta + K_{X_0}{}^2\sin^2\eta\right)^{1/2}$
K_{XZ}	nondimensional product-of-inertia parameter, $\left(K_{Z_0}{}^2 - K_{X_0}{}^2\right)\sin\eta\cos\eta$
C_W	weight coefficient, W/qS
C_D	drag coefficient, Drag force/qS
C_Y	lateral-force coefficient, Lateral force/qS
C_l	rolling-moment coefficient, Rolling moment/qSb

C_n yawing-moment coefficient, Yawing moment/qSb

C_{l_β} effective-dihedral derivative, rate of change of rolling-moment coefficient with angle of sideslip, per radian

C_{n_β} directional-stability derivative, rate of change of yawing-moment coefficient with angle of sideslip, per radian

C_{Y_β} lateral-force derivative, rate of change of lateral-force coefficient with angle of sideslip, per radian

C_{n_r} damping-in-yaw derivative, rate of change of yawing-moment coefficient with yawing-angular-velocity factor, per radian

C_{n_p} rate of change of yawing-moment coefficient with rolling-angular-velocity factor, per radian

C_{l_p} damping-in-roll derivative, rate of change of rolling-moment coefficient with rolling-angular-velocity factor, per radian

C_{l_r} rate of change of rolling-moment coefficient with yawing-angular-velocity factor, per radian

C_{Y_δ} rate of change of side-force coefficient with angle of control deflection, per radian

K control gearing ratio of autopilot sensitive to transverse velocity or acceleration, $\frac{\text{radians}}{\text{ft/sec}}$ or $\frac{\text{radians}}{\text{ft/sec}^2}$

$K' = KVC_{Y_\delta}$

$A_0, A_1, \ldots A_5$ coefficients of the stability equation

P period of oscillation, sec

$T_{1/2}$ when positive, time required for a stable motion to damp to one-half amplitude; when negative, time required for an unstable motion to double amplitude; sec

s_b nondimensional time parameter, Vt/b

D_b differential operator, d/ds_b

Subscript:

o	initial

Towline terms:

T	towline tension, $\text{Drag}/\cos \zeta$, lb
C_T	towline tension coefficient, $C_D/\cos \zeta$
ζ	angle between towline and relative wind, positive when towline is above relative wind, deg (fig. 2)
x	distance along X-axis from center of gravity of fighter to towline attachment point, positive forward of center of gravity, spans (fig. 2)
z	distance along Z-axis from center of gravity of fighter to towline attachment point, positive above center of gravity, spans (fig. 2)
y	sidewise movement of center of gravity along Y-axis, ft
y'	nondimensional sidewise movement of center of gravity along Y-axis, spans
l	towline length, spans
$T_{y_{y'}}$	rate of change of lateral force caused by towline tension with sidewise displacement
T_{y_ψ}	rate of change of lateral force caused by towline tension with angle of yaw
T_{y_ϕ}	rate of change of lateral force caused by towline tension with angle of bank
$T_{n_{y'}}$	rate of change of yawing moment caused by towline tension with sidewise displacement
T_{n_ψ}	rate of change of yawing moment caused by towline tension with angle of yaw
T_{n_ϕ}	rate of change of yawing moment caused by towline tension with angle of bank
$T_{l_{y'}}$	rate of change of rolling moment caused by towline tension with sidewise displacement

T_{l_ψ} rate of change of rolling moment caused by towline tension with angle of yaw

T_{l_ϕ} rate of change of rolling moment caused by towline tension with angle of bank

ANALYSIS

Equations of Motion

The equations of motion for the lateral motion of a towed airplane have been derived in references 1 and 2, and the characteristic equation of the lateral motion has been shown to be of sixth degree. The assumptions and the methods of derivation used in references 1 and 2 are similar. The fundamental assumptions are that the disturbance of the motion of the towing airplane is negligible, that the disturbed motion of the towed airplane is small enough to permit the equations of motion to be linearized, and that the dynamic properties of the towline may be neglected.

Except for differences in notation and several typographical errors, the equations of motion used in references 1 and 2 are essentially the same. The notation used in the present paper is that of reference 2, and the slight discrepancies between the equations here presented and those of reference 2 arise from the previously mentioned typographical errors. The nondimensional equations of motion in sideslip, yaw, and roll for small disturbances from level flight may be written as follows:

$$\left(2\mu_b D_b^2 - C_{Y_\beta} D_b - T_{y_{y'}}\right)\beta + \left(2\mu_b D_b^2 - T_{y_\psi} D_b - T_{y_{y'}}\right)\psi - \left(C_W + T_{y_\phi}\right) D_b \phi = D_b C_Y \tag{1}$$

$$-\left(C_{n_\beta} D_b + T_{n_{y'}}\right)\beta + \left(2\mu_b K_Z^2 D_b^3 - \frac{1}{2} C_{n_r} D_b^2 - T_{n_\psi} D_b - T_{n_{y'}}\right)\psi +$$

$$\left(2\mu_b K_{XZ} D_b^2 - \frac{1}{2} C_{n_p} D_b - T_{n_\phi}\right) D_b \phi = D_b C_n \tag{2}$$

$$-\left(C_{l_\beta}D_b + T_{l_{y'}}\right)\beta + \left(2\mu_b K_{XZ} D_b^3 - \frac{1}{2}C_{l_r}D_b^2 - T_{l_\psi}D_b - T_{l_{y'}}\right)\psi +$$

$$\left(2\mu_b K_X^2 D_b^2 - \frac{1}{2}C_{l_p}D_b - T_{l_\phi}\right)D_b\phi = D_b C_l \tag{3}$$

The towline derivatives $\left(T_{y_{y'}}, T_{y_\psi}, \text{etc.}\right)$ which occur in these equations are defined in terms of the towline tension coefficient C_T, the towline length l, the coordinates x and z of the towline connection point in the stability system of axes, and the towline inclination ζ with respect to the undisturbed velocity. The towline parameters are shown in figure 2. All lengths are given nondimensionally in wing spans.

The tension coefficient is given in terms of the drag coefficient and the towline inclination as

$$C_T = \frac{C_D}{\cos\zeta} \tag{4a}$$

Moreover, the weight coefficient $C_W \equiv \frac{W}{qS}$ is not the same as the lift coefficient when $\zeta \neq 0$, since there is a vertical tension force in this case. The proper relation is

$$C_T \sin\zeta = C_W - C_L \tag{4b}$$

The usual relation for level flight, $C_L = C_W$, is valid when $\zeta = 0$.

The towline derivatives are expressed in terms of towline parameters as follows:

$$T_{y_{y'}} = -\frac{C_T}{l} \tag{5}$$

$$T_{n_{y'}} = xT_{y_{y'}} = -x\frac{C_T}{l} \tag{6}$$

$$T_{l_{y'}} = zT_{y_{y'}} = -\frac{zC_T}{l} \tag{7}$$

$$T_{y_\psi} = -C_T\left(\frac{x}{l} + \cos\zeta\right) \tag{8}$$

$$T_{n_\psi} = xT_{y_\psi} = -xC_T\left(\frac{x}{l} + \cos\zeta\right) \tag{9}$$

$$T_{l_\psi} = zT_{y_\psi} = -zC_T\left(\frac{x}{l} + \cos\zeta\right) \tag{10}$$

$$T_{y_\phi} = -C_T\left(\frac{z}{l} + \sin\zeta\right) \tag{11}$$

$$T_{n_\phi} = xT_{y_\phi} = -xC_T\left(\frac{z}{l} + \sin\zeta\right) \tag{12}$$

$$T_{l_\phi} = zT_{y_\phi} = -zC_T\left(\frac{z}{l} + \sin\zeta\right) \tag{13}$$

Here x is positive when the connection is ahead of the center of gravity, z is positive above the center of gravity, and ζ is positive when the cable is inclined up (towing airplane higher than the towed airplane).

Characteristic Equation and Characteristic Modes

The characteristic equation corresponding to equations (1), (2), and (3) seems to be of eighth degree with no constant coefficient (that is, one root is identically zero). However, by means of the definitions of the towline derivatives, it can be shown that the first power term in D_b also vanishes identically. These two zero roots have been introduced by differentiating each equation once, and the characteristic equation is therefore actually of sixth degree. This equation has the form

$$D_b^6 + A_5 D_b^5 + A_4 D_b^4 + A_3 D_b^3 + A_2 D_b^2 + A_1 D_b + A_0 = 0 \tag{14}$$

The expressions for the coefficients of this equation are given in the appendix.

As discussed in part IV of reference 1, the new characteristic mode, which is introduced when the lateral characteristic equation of fourth degree for the free airplane is increased to sixth degree by the addition of the towline, is an oscillation. The free lateral oscillation, generally called the Dutch roll, and the heavily damped aperiodic mode, generally called the damping-in-roll mode, usually remain practically unchanged when the towline is added. However, the usual lightly damped aperiodic mode, generally called the spiral mode, is very strongly affected by the addition of the towline. In fact, it seems that, when the towline is added, the spiral mode for the free airplane is usually replaced by a combination of the new oscillation and an aperiodic mode which may be heavily damped.

The new oscillation will be called the towline oscillation. It should be remembered, however, that this is an airplane motion, not a towline motion. Physically, this oscillation appears to be caused by the tension force in the towline, which tends to return the airplane to equilibrium when the point of attachment undergoes a lateral displacement. The closely related aperiodic mode will be called the towline aperiodic mode. The relation between the towline modes and the free spiral mode may be explained by considering the coefficient A_5 of equation (14). The magnitude of this coefficient is a measure of the total damping of the system. As can be seen in the appendix, however, this coefficient does not contain any towline terms; that is, the total damping of the characteristic modes is the same for the free or towed airplane. Since the Dutch roll and damping in roll are usually little affected by the addition of the towline, the damping of the spiral mode must be shared by the two towline modes. Since the free-airplane spiral mode has little damping, however, it follows that when the towline aperiodic mode is heavily damped, the towline oscillation will be correspondingly unstable.

Necessity for Calculating Motions

There is a theoretical objection to placing too much reliance on the characteristic roots alone. In setting up the equations of motion, the assumption of small motions was used in order to obtain linear equations. Roughly, this assumption may be said to require that the angle between the towline and the steady-state flight direction may be used to replace the sine of the angle in addition to the usual requirements for the motion of a free airplane. The sine of an angle is approximately equal to the angle up to about $\pi/6$ radians. Thus, the assumption requires that the sidewise displacement of the towed airplane become no larger than half the towline length. For motions of this magnitude, the characteristic roots and calculated motions obtained from the linearized equations of motion may be considered approximately correct. However, the magnitude of the sidewise motion clearly depends on the type and magnitude of disturbance assumed (that is, the applied forces and initial conditions). In analyzing any type of stabilization method, it is therefore necessary to calculate not only the characteristic roots but also actual motions following reasonable types of disturbances. If the sidewise displacement is calculated to be greater than half the towline length or if any other degree of freedom becomes too large, the whole analysis is of doubtful validity since the motions contradict the assumptions used to calculate them.

Three types of disturbance were considered in obtaining the motions for the stabilization devices considered. These disturbances corresponded to a 2° rudder kick held for 1 second, an initial sideslip angle of 2° (which corresponds to an initial sidewise velocity of approximately 35 mph), and an initial yawed position in which $\psi_o = -5^\circ$ and $\beta_o = 5^\circ$. The choice of the types and magnitudes of the disturbances was rather arbitrary, but it is felt that they give a reasonably accurate representation of the types of disturbance which might occur. The 2° rudder kick, held for 1 second, is clearly a reasonable type of disturbance, since it is the type that a pilot would probably use in testing the stability of the towed airplane. For this reason, most of the emphasis will be on this disturbance, and the other motions will be used chiefly for comparison. All motions were obtained by use of a Reeves Electronic Analog Computer.

RESULTS

No attempt is made in the present paper to carry out a thorough investigation of any particular method of stabilizing the lateral motion of a towed fighter airplane. Rather is this a preliminary investigation, whose chief purpose is to find and compare roughly several possible methods of stabilization so that the way may be open for further research into the more promising methods. Therefore only a single flight condition of a hypothetical fighter will be chosen as the basic airplane configuration which is being towed. Various methods will be investigated for stabilizing this basic condition without considering whether these methods would be effective in other flight conditions. There is, however, no obvious reason why a method which is effective in stabilizing this typical flight condition would not also be effective in other flight conditions or for other airplanes. In particular, since the previous research on towed gliders has emphasized the fact that for increased relative-density parameter μ_b the lateral stability tends to decrease, the methods which appear effective in stabilizing the towed fighter, which has high μ_b, should also be effective when applied to gliders.

The mass and aerodynamic parameters of the hypothetical fighter are given in table I. The corresponding characteristic modes are presented in the first row of table II. It should be noted that the spiral mode is very slightly stable.

Influence of Towline Parameters

Before the use of automatic controls was investigated, the possibility of stabilizing the configuration by varying towline parameters only was considered. The first step was to investigate the effect of attaching the towline to the fighter in some simple manner. It was assumed that the towline was attached to the nose of the airplane, and $\zeta = 0$ was chosen in order to obtain the simple relation $C_L = C_W$. As a reasonable basic length for the towline, $l = 1{,}000$ feet (26 spans) was assumed. The angle of attack calculated for level flight was $\alpha = 2.4^\circ$. In the stability system of axes, the corresponding connection point (connection at the nose) was $z = 0.022$ span and $x = 0.52$ span. This case, then, was assumed as the basic case in which various parameters might be varied in an attempt to obtain stability.

Effect of towline parameters on characteristic modes.- To obtain the characteristic modes, the required parameters were inserted into the expressions for the coefficients given in the appendix, and the roots of the characteristic sextic were obtained. The corresponding characteristic modes for the basic case are given in row 2 of table II. Comparison of these modes with those of the airplane alone reveals that the Dutch roll mode and the damping-in-roll mode are scarcely changed. The towline aperiodic mode is very stable, and the towline oscillation is correspondingly unstable. As was previously pointed out, the reason for this distribution of damping is that the total towline-mode damping must equal the spiral damping when the Dutch roll and damping in roll are not appreciably changed by the towline.

The first parameter to be varied was the towline length. Rows 3, 4, 5, and 6 of table II show the characteristic modes for $l = 2.6$, 13, 130, and ∞ (in spans), respectively. The period and damping of the towline oscillation both increase with length. The most interesting result is that increasing towline length has a stabilizing effect on the towline oscillation, and for infinite length the motion is stable. Even for 5,000 feet (l = 130 spans), however, the towline oscillation is still unstable, so that it would appear impractical to attempt to achieve stability simply by increasing the towline length.

Another method for stabilizing the towline oscillation is suggested by the form of the constant coefficient A_0 in the appendix. If varying the towline parameters has little effect on the Dutch roll or damping-in-roll modes, then the damping of the towline oscillation should be improved if the towline parameters can be varied so as to decrease the towline aperiodic damping. This possibility follows from the fact that the sum of the towline dampings is approximately equal to the spiral damping. From the form of A_0 it is clear that A_0 must vanish when $\frac{z}{x} = \frac{C_{l_\beta}}{C_{n_\beta}}$. It follows that this condition should give a stable oscillation, since vanishing A_0 corresponds to a neutrally stable towline aperiodic mode. The value $z = -0.0805$ span makes $A_0 = 0$. Row 7 of table II shows the characteristic modes for $z = -0.0804$ span, and the predicted stability for the towline oscillation is seen to occur. It is interesting to note that the characteristic modes of this configuration are very similar to those of the basic case with infinite length.

The case of $z = -0.0804$ span corresponds to an attachment point somewhat less than 4 feet down from the nose. The characteristic modes obtained with this attachment point indicate that the lateral stability would be reasonably satisfactory. The Dutch roll oscillation and the damping-in-roll mode are practically unchanged from those of the free airplane; and the lightly damped long-period oscillation, in combination with the lightly damped aperiodic mode, would probably have much the same effect as the original lightly damped spiral mode. However, it will be shown that the attainment of stability by this adjustment of z is impractical because of the extreme sensitivity of the stability to changes in z.

Previous unpublished experimental results had indicated that large positive values of z for the attachment point had given a stable configuration. In order to investigate this possibility, the coefficients of the characteristic equation were written as functions of z, and Routh's discriminant for this equation was obtained as a function of z. An analysis of the roots of Routh's discriminant indicated that the towline oscillation would become unstable for values of z above -0.0796 span but would become stable again at values of z between 2.374 spans and 3.851 spans. The characteristic modes were obtained for $z = 2.5$ spans and $z = 3.0$ spans and were found to be satisfactory. Row 8 of table II shows the characteristic modes for $z = 3.0$ spans. Although there is a large range of positive z values which give stability, this range occurs at values of z which are impractically large, since almost a 90-foot mast would be required.

The stable range of negative z values, on the other hand, occurs at reasonably small values. However, since the real mode is unstable at values of z below $z = -0.0805$ span and the towline oscillation is unstable for values above $z = -0.0796$ span, the stable range is only 0.4 inch. This stable range for negative z is too narrow to be practical. There is, therefore, no practical range of z values which yields a stable configuration for the present case. Some possibility exists, however, that the other parameters, for example, ζ, might be adjusted to make the stable z range more practical.

Unlike the small negative value of z used to obtain stability, the large positive values seem to have a considerable effect on the Dutch roll and damping-in-roll modes. No attempt was made to analyze these effects, since the total motion was stable.

Previous investigators (for example, ref. 1) have mentioned that attaching the cable at the center of gravity usually gives a stable configuration. Although it would be impossible to attach the cable exactly at the center of gravity, it might be practical to use an attachment point near the center of gravity. The characteristic roots that correspond to a connection at the center of gravity are shown in row 9 of table II. The Dutch roll and damping-in-roll modes are practically unchanged from those of the free airplane and the long-period, lightly damped towline mode is very little different from the lightly damped spiral mode of the free airplane. It is interesting to note that the case of the center-of-gravity connection, the case of $l = \infty$, and the case of $z = -0.0805$ span all give a fifth-degree equation, rather than the usual sixth-degree equation; and these three cases also are all stable.

In a more thorough investigation it would be desirable to investigate the effect of varying ζ. However, because of the extremely large number of variables which could be considered in attempting to improve the stability of the towed fighter, it was necessary almost arbitrarily to choose certain variables on which to concentrate in a preliminary analysis, The investigation of the variation of ζ would have required the calculation of many more cases. Moreover, since large values of ζ would cause increased cable drag at high speed and since there was no obvious reason why extremely favorable results should be obtained by varying ζ, no such variation was considered. The results of rows 7, 8, and 9 in table II are sufficient to establish the fact that it is theoretically possible to obtain complete stability with adjustment of towline parameters only.

Calculated motions.- For comparison, the motions of a free airplane subsequent to the three types of disturbance are shown in figure 3. The motions in sideslip, sidewise displacement, and bank angle are presented. Although the sidewise displacement is of no importance in a stability analysis of a free airplane, the tendency to sidewise displacement becomes important when the airplane is being towed. The disturbance consisting of an initial sidewise velocity (fig. 3(b)) gives the largest sidewise motion, as might be expected. The motion called sidewise displacement, denoted by the symbol y on the figures, is actually $V\int(\psi + \beta)dt$, and would more accurately be called the transverse displacement. For small angles of bank this can be seen to be essentially sidewise motion. However, the direction of this motion actually makes an angle ϕ with the horizontal at any instant, so that a varying amount of gravity force is applied along the direction of this motion depending on the angle of bank. This is the C_W term in equation (1). The importance of this term will appear in later discussion.

Motions were next obtained for the basic case of a nose attachment. These are presented in figure 4. The presence of the Dutch roll mode and the highly unstable towline oscillation predicted in table II, row 2, is evident. As usual, there is very little of the Dutch roll mode in the transverse displacement. The transverse displacement seems to be determined mainly by the characteristic towline oscillation. The rolling motion also depends strongly on the characteristic towline oscillation, particularly in the response to a sideslip disturbance.

Figures 5(a) and 5(b) show the responses to the rudder kick and sideslip disturbance, respectively, when the point of attachment is at $z = -0.0804$ span. Since the third initial condition ($\psi_o = -5^\circ$ and $\beta_o = 5^\circ$) consistently shows smaller motions than the other two, it will be ignored in future considerations. As predicted, the towline oscillation is stable, and this long-period oscillation would probably not be very troublesome to a pilot. It seems significant that this proper choice of z for stability causes an enormous decrease in the relative amount of rolling motion present in the towline oscillation.

The motions which have been presented seem to indicate that the lateral towline oscillation is essentially a transverse oscillation of the whole airplane, in which, however, the rolling motion and rolling moments may be important. The motion in figure 4(b) is not correct for the large bank angles, but this fact is not important since it is sufficient to know that extreme instability and a tendency to very large bank angles exist in this case.

Effects of Modifying Stability Derivatives by Automatic Control

Variation of C_{l_r} to increase spiral damping.- It seemed reasonable to suspect that the smallness of the stable range of negative values of z

arose from the fact that the damping of the free-airplane spiral mode was very small. The damping of the spiral mode may be increased by making C_{l_r} more negative, as shown in reference 3. This type of C_{l_r} variation would tend to have an adverse effect on the Dutch roll damping, but this could be taken care of by simultaneously making C_{n_r} more negative. Such an autopilot would feed yaw-rate signals to both rudder and ailerons. In this work it was always assumed that the autopilots had no lags, so that the effect of the autopilot is considered simply as a modification of the stability derivatives.

Increments in both stability derivatives were considered in the vicinity of the value -1.5. Although there was a considerable increase in the amount of damping of the towline modes, no significant increase in the range of negative values of z giving a stable configuration was found. For this reason the detailed results are not presented,

Consideration of towline oscillation as an oscillation in transverse displacement.- The calculated motions seemed to indicate that the towline oscillation contained a good deal of transverse displacement of the whole airplane and a large amount of rolling motion. The choice of z which tended to increase the damping of the towline oscillation also greatly decreased the amount of rolling motion. If the towline oscillation is considered to be primarily an oscillation in transverse displacement, then the velocity of the equivalent oscillator is the transverse velocity $V(\psi + \beta)$. To damp the oscillator it is necessary to introduce a control-surface deflection which opposes the transverse motion and is proportional to the transverse velocity. It would seem reasonable to use a rudder-type control surface to oppose the transverse motion. Usually only the yawing moment caused by such a control is considered and the side force is ignored. The importance of lateral displacement in developing towline forces, however, makes it desirable to consider the side force developed by the control surface in the present problem. In order to determine whether the side force developed by deflecting the control surface could have an important effect on the stability, only side forces were assumed to be obtained from the control surface.

The control equation is

$$\delta = KV(\psi + \beta) \tag{15}$$

The input for such an autopilot could be obtained by integrating the signal from a lateral accelerometer. When only side forces are considered, a term $C_{Y_\delta} D_b \delta$ is included on the right-hand side of equation (1). In order to avoid the necessity of estimating a value of C_{Y_δ} for the control surface, the parameter $C_{Y_\delta}\delta$ was plotted instead of δ. From equation (15), if $K' = KVC_{Y_\delta}$, then

$$C_{Y_\delta}\delta = K'(\psi + \beta) \tag{16}$$

Row 10, table II, shows the characteristic modes when this type of autopilot is applied to the basic configuration with $K' = -1.92$. A comparison of these modes with those of the basic case indicates that both the oscillatory and aperiodic towline modes have better stability, but the oscillatory towline mode is still unstable. As in the basic case, this instability could be removed by adjusting z. Row 11, table II, gives the characteristic modes with this autopilot and $z = -0.0805$ span. The towline oscillation is very stable and its period is very long. These results indicate that control side force alone can have an important effect on the stability and should therefore be included in considering any autopilot. Because of the desirable nature of the characteristic modes, it was decided to calculate motions with the side-force automatic control. Motions were obtained for several values of z and K', and the parameter $C_{Y_\delta}\delta$ was plotted in addition to the other variables. In this way, it could be determined whether the necessary values of K' required too large δ motions for reasonable values of C_{Y_δ} and, also, whether a reasonable range of z values could be used.

The motion for $K' = -1.92$ and $z = -0.0804$ span is shown in figure 6. Figure 6(a) shows the response to the rudder kick, and figure 6(b) shows the response to initial sideslip. The towline oscillation is practically deadbeat. To obtain the value of δ (in degrees) at any time, it is necessary to divide the value of $C_{Y_\delta}\delta$ by the value of C_{Y_δ} (per radian) of the control surface. From figure 6(a), if the magnitude of C_{Y_δ} is 0.02, then the maximum magnitude of δ is less than 20°. Since it is reasonable to expect that control surfaces with $|C_{Y_\delta}| \geqq 0.02$ can be used, the required gain does not call for excessive control deflection. For the initial sideslip, on the other hand, figure 6(b) shows that large values of transverse displacement and control deflection occur. In actual flight, however, it seems doubtful that such large sideslip velocities would suddenly occur as are assumed in this initial condition. Moreover, the motions develop so slowly that it is probable that the pilot could take corrective action before the motions became too large. In the subsequent figures only the response to the rudder kick is shown, since this is clearly a physically realistic disturbance. In every case the sideslip response gives rise to larger motions, such as are shown in figure 6(b).

The motion following a rudder kick for $z = -0.0740$ span and $K' = -1.92$ is shown in figure 7. Although the very long period oscillation is now noticeable, the motion is clearly stable and satisfactory. This motion corresponds to a change of 3 inches in the value of z from that used for the motions in figure 6. In figure 8 the motion is shown when z has been changed by 1 foot, to $z = -0.0544$ span. Although the towline oscillation is neutrally stable, it would probably be easily controllable because of its long period. It therefore seems that this large autopilot gain would give adequate stability for a range of z values of approximately 1 foot, which is a practically useful range. Although a control surface which gives only side force is clearly impractical, it may be approximated by placing the control as near the center of gravity as possible. The small moments caused by the control may then be chosen so that they do not decrease the stability.

When the magnitude of K' was reduced, the principal effects were a decrease in towline oscillation stability and a slight decrease in control motion. For $K' = -1.0$ the towline oscillation was still rather stable at $z = -0.0740$ span. For $K' = -0.5$ the oscillation was neutrally stable at $z = -0.0740$ span. For this smaller gain, the stable range of z has decreased to 3 inches. Since no significant changes in the motion occurred other than those mentioned, the motions are not shown.

The investigation of the automatic control which applied side force only was begun mainly to see whether the side force developed by a rudder-type control surface might have an important effect on the stability. It was extended because of the desirable type of towline oscillation which resulted from this type of control. In considering the effect of both yawing moment and side force of the control surface on the stability of the towline oscillation, calculations were made by a method of slopes similar to that described in reference 4. The calculations indicated that a forward position of the control surface would be desirable. The control surface was therefore assumed to be at the nose. If the control surface is assumed to be below the nose, the control rolling moment is practically zero. This assumption was made for simplicity. The control yawing moment was introduced into the equations of motion by adding a term $\frac{l_A}{b} C_{Y_\delta} D_b \delta$ on the right-hand side of the yaw equation, where l_A is the distance along the X-axis between the control surface and the center of gravity. Otherwise, the equations of motion are the same as those for the side-force control.

The characteristic modes resulting from the use of this autopilot in the basic configuration are shown in row 12 of table II. The towline oscillation is very stable, but two undesirable effects are apparent: The period of the towline oscillation is greatly decreased and the damping of the Dutch roll mode is decreased. The damping of the Dutch roll mode may be improved by an ordinary yaw-damper. However, the decrease of the towline oscillation period could cause serious difficulties if this period came close to the period of the characteristic lateral oscillation of the bomber. In this event, relatively large bomber motions might result, and the assumption that the dynamics of the bomber may be neglected would break down. To determine whether the effect of the bomber motion would be harmful or beneficial to the total stability would require a more complicated analysis. In the present paper it is only desired to point out that when the present analysis gives an oscillatory mode with a period close to that of the bomber, the validity of the whole analysis becomes doubtful.

By assuming that the bomber motion is not of sufficient importance to invalidate the analysis, motions were obtained with this autopilot. The motion in figure 9 is for $K' = -1.92$ and $z = 0.022$ span, subsequent to a rudder kick. The motion obtained with this autopilot is not only stable but also has the desirable property that its magnitude is quite small. Figure 10 shows the motions for the same autopilot for towline connection at $z = -0.0804$ span. It is interesting to observe that the motion is almost identical with that shown in figure 9. Thus, this autopilot seems to have the very desirable property that its effect depends very little on the towline attachment point.

The motion in figure 11 is for a nose attachment with $K' = -1.0$. Comparison with figure 9 shows that the decrease of gearing ratio results in a decrease of damping for the towline oscillation and an increase in period. The motion for $z = -0.0804$ with $K' = -1.0$ is almost identical with that shown in figure 11 for the nose connection, and is therefore not shown.

Stabilization by roll control.- It has been shown that the stability of the towline oscillation could be improved simply by adjusting z. The variation of z causes a variation of the rolling moment caused by the towline. It might therefore be surmised that an aileron-type automatic control might improve the stability of the towline oscillation. Moreover, as has previously been mentioned, there is often a good deal of rolling in the towline oscillation. This oscillatory variation of angle of bank causes an oscillatory variation of the transverse component of the weight. The phase relation between this oscillatory transverse force and the transverse displacement can clearly be very important in determining the magnitude of this displacement. Therefore the proper type of roll control might also be effective in reducing the magnitude of the towline oscillation.

The original plans for this preliminary analysis did not include an investigation of roll controls, since several different types would have to be considered. However, some unpublished experimental work had shown that it was possible to stabilize a free-flying model, which was fastened in a wind tunnel by a simple cable, when an autopilot providing rolling moments proportional to angle of bank was used. Unpublished experimental results for zero towline length had also indicated that spring restraint in roll stabilized the lateral motion. It was therefore decided to investigate the effect of an autopilot which would provide a rolling moment proportional to angle of bank.

The characteristic modes obtained with such an autopilot were calculated by assuming increments in T_{l_ϕ}. The increments used were -0.015, -0.025, -0.050, and -0.100. Within this range the system was stable and the variation of the autopilot effectiveness caused little significant change in the characteristics of the system. Rows 13 and 14 of table II show the characteristic roots for increments $\Delta T_{l_\phi} = -0.015$ and $\Delta T_{l_\phi} = -0.100$, respectively. The characteristic roots for $\Delta T_{l_\phi} = -0.050$ were obtained for both the basic case (z = 0.022 span) and the case of z = -0.0804 span. The roots were found to be practically identical.

The motions for $\Delta T_{l_\phi} = -0.025$ and $\Delta T_{l_\phi} = -0.050$ are presented in figures 12 and 13, respectively. There is little change in the type of motion when the autopilot effectiveness is doubled. Although the towline oscillation is only slightly stable, the period is so long and the motion (in response to the 1-second, 2° rudder kick) is so small that this type of control seems to be very satisfactory. No δ-motion was obtained in this case because the increments in T_{l_ϕ} assumed can be shown to require only small control deflections. The autopilot assumed here would deflect an aileron-type auxiliary surface proportionately to the angle of bank as obtained from a position gyro or by integration of a roll-rate gyro signal.

Some of the apparent advantages of this type of control are: small autopilot power required, small motions in response to disturbances, long-period towline oscillation, possibility of improving the Dutch roll stability, and lack of sensitivity to changes in gearing ratio of the autopilot or point of towline attachment.

DISCUSSION OF RESULTS

The results obtained by considering the variation of towline parameters are generally in qualitative agreement with the results of previous investigations on towed gliders. The stabilizing effect of increased towline length or attachment near the center of gravity has long been known for towed gliders. The use of a bridle-type connection, attached to both sides of the fuselage at x = z = 0, would seem to be a practical method of approximating a center-of-gravity attachment. This method of stabilization seems to merit further research.

For the nose attachment, the calculated motion shows that the unstable towline oscillation is a violent "swooping" type of oscillation, involving a large amount of rolling of the airplane. At the extreme values of sidewise displacement the angle of bank is practically zero, and it has maximum magnitude when the sidewise displacement is near zero. It is interesting to note that the bank introduces a weight force in the proper phase to augment the motion.

Apparently, the adjustment of the z/x ratio so that $\frac{z}{x} = \frac{C_{l_\beta}}{C_{n_\beta}}$ causes some sort of balance between the towline forces and aerodynamic forces which tends to keep the rolling motion small. The adjustment of z/x makes it possible to distribute the damping of the towline aperiodic and oscillatory modes. Although the mathematical reason for this is fairly clear, the physical reason is rather obscure. The physical reason for the stabilizing effect of large z values is probably the introduction of relatively large negative values of $T_{l\phi}$. This would indicate that using a large inclination angle ζ might make this type of stabilization possible with smaller z values. (See equation (13).). Also, the use of positive values of z for stabilization might be relatively more effective at shorter cable lengths. In this case, however, it is necessary to consider that the decrease in cable length itself has a somewhat destabilizing effect.

The physical reason for the effectiveness of the autopilots which apply some sort of restoring force or moment, or both, proportional to sidewise velocity is fairly clear. Both the autopilot which applies side force only and that which includes yawing moments seem to provide possible practical methods of stabilization. If the side-force autopilot is used, it will probably be necessary to adjust the z/x ratio also. The rudder-type control seems more practical and it does not require the z/x adjustment. In this case, however, the possible effects of the short period of the towline oscillation must be considered. Because of the large change in towline oscillation period caused by this autopilot, there is reason to believe that a phase-shift network which introduces some phase lead into the activating signal of the autopilot would be beneficial. If the towline oscillation is considered as an independent oscillator, then it would seem that the restoring force applied by the autopilot is not in phase with either the velocity or the displacement of the oscillator but must instead lie somewhere between these two since it increases both frequency and damping. For this reason, an activating signal which leads the sidewise velocity would seem preferable.

A simple way to check this conjecture seemed to be to obtain the characteristic roots when an autopilot sensitive to sidewise acceleration was used rather than one sensitive to sidewise velocity. The characteristic modes for this case were obtained for $K' = -1.92$ seconds, and are presented in row 15 of table II. The fact that damping has been added to the towline oscillation while the period has been lengthened seems to confirm the physical reasoning that an autopilot which responds to a signal whose phase is intermediate between that of the transverse velocity and that of the acceleration could improve the damping of the towline oscillation without shortening its period. Such an autopilot could be obtained by simply replacing the integrating device previously used with the accelerometer by a device providing a phase lag somewhere between 0° and 90°. Actually, the modes obtained by using the accelerometer itself would be satisfactory if the calculated motions are not too large for the assumptions of linearity.

In considering the rudder-type autopilot, the rolling moments caused by the control surface were neglected. This was possible in the particular case considered because the center of pressure of the control surface below the nose would fall almost exactly on the X-axis. In order to obtain a qualitative idea of the effects of rolling moment in the more general case, the method of slopes was applied to investigate the sensitivity of the towline oscillation mode to changes in C_{l_β} and T_{l_ψ}. When the results are compared with the slopes obtained from the yawing-moment derivatives, the towline oscillatory mode appears to be considerably more sensitive to the rolling moment due to sidewise velocity than it is to the yawing moment due to sidewise velocity. Moreover, there is a physical argument which tends to bear out the conclusion that a negative rolling moment due to sidewise velocity should be effective in stabilizing the towline oscillation.

In comparing the various motions presented, it is seen that the motions obtained with the rudder-type autopilot and the T_{l_ϕ} autopilot are smaller in magnitude than any of the motions obtained with the other autopilots. The reason for these small amplitudes seems to be that the phase relation between bank angle and sidewise motion in these two cases is different from that in any of the other cases. In these two cases the bank angle is largest near the peaks of the sidewise motion and is in the proper direction to introduce a weight force opposing this motion, whereas in the other cases the bank angle tends to augment the sidewise motion, as previously described. In considering the effect of rolling moment proportional to sidewise velocity, it can be seen that a negative rolling moment in response to sidewise displacement should tend to prevent the build-up of the bank angle which would augment the sidewise motion. Since this physical argument is in agreement with the result predicted by the method of slopes, it appears that in the general case the rolling moment caused by the control surface should not be neglected. In fact, the use of an auxiliary surface below the rudder might be very effective in improving the damping of the towline oscillation.

In investigating the effect of rolling moments, it was found that a very small positive increment in C_{l_β} would yield a considerable improvement in the stability of the towline oscillation while also increasing the period. The reason for this seems to be that z/x for the nose connection is a small positive value and the condition $\frac{z}{x} = \frac{C_{l_\beta}}{C_{n_\beta}}$, which has been shown to be stabilizing, is approached when C_{l_β} is given a positive increment. The stabilizing effect of the use of zero C_{l_β} rather than a negative value for towed airplanes is particularly interesting because of the recent tendency toward small values of effective dihedral. In particular, the use of a bridle connection at the center of gravity of an airplane for which C_{l_β} is zero would seem to be very promising.

Finally, on the basis of the motions actually calculated in the present investigation, the autopilot that provides rolling moments proportional to bank angle seems to give the most desirable results. The autopilot is simple, the motions are small, there is little sensitivity to changes in gearing or point of connection, and the towline oscillation period is so long that there seems little doubt of the validity of the initial assumptions.

CONCLUDING REMARKS

The lateral motion of a high-speed fighter airplane towed behind a high-speed bomber by means of a single towline is shown to be very unstable. A number of possible methods for stabilizing the lateral motion of the towed fighter are presented in this preliminary investigation. Of the methods presented, the two which show most promise of being practical require the use of automatic control. One method requires an autopilot providing aileron deflection proportional to angle of bank, and the other requires an autopilot providing deflection of a rudder-type control surface proportional to a linear combination of transverse acceleration and velocity. The possibility of obtaining stability by adjustment of towline parameters only is not dismissed, however. In particular, the use of a center-of-gravity towline connection merits further research.

Since previous investigators have shown that the lateral motion of a towed aircraft is more difficult to stabilize than the longitudinal motion, the results of this analysis indicate that the use of a simple tow cable may be a practical method of increasing the range of a high-speed fighter. In view of the simplicity of this method in comparison with the other methods which have been tried, a more thorough experimental and analytical investigation of this method would seem desirable.

Langley Aeronautical Laboratory,
National Advisory Committee for Aeronautics,
Langley Field, Va.

APPENDIX

EXPRESSIONS FOR COEFFICIENTS OF THE CHARACTERISTIC EQUATION

FOR THE LATERAL MOTION OF A TOWED AIRPLANE

The coefficient of the highest-degree term in the characteristic equation is $8\mu_b{}^3\left(K_X{}^2K_Z{}^2 - K_{XZ}{}^2\right)$. The error introduced by neglecting the $K_{XZ}{}^2$ term in this expression is negligible. As in reference 1, the approximation $K_X{}^2K_Z{}^2 - K_{XZ}{}^2 \approx K_X{}^2K_Z{}^2$ will therefore be used. The characteristic equation is then divided through by the leading coefficient and takes the form given in equation (14). The expressions for the coefficients in equation (14) then become

$$A_0 = \frac{C_T C_W\left(zC_{n_\beta} - xC_{l_\beta}\right)}{8\mu_b{}^3 l K_X{}^2K_Z{}^2}$$

$$A_1 = \frac{C_T}{8\mu_b{}^3 l K_X{}^2K_Z{}^2}\left\{\frac{1}{2}\left(C_{l_\beta}C_{n_p} - C_{n_\beta}C_{l_p}\right) + z\left[C_W C_{n_\beta}(x + l\cos\zeta) - \frac{1}{2}\left(C_W C_{n_r} + C_{Y_\beta}C_{n_p}\right)\right] + x\left[\frac{1}{2}\left(C_W C_{l_r} + C_{Y_\beta}C_{l_p}\right) - C_W C_{l_\beta}(x + l\cos\zeta)\right]\right\}$$

$$A_2 = \frac{C_W\left(C_{l_\beta}C_{n_r} - C_{n_\beta}C_{l_r}\right)}{16\mu_b{}^3K_X{}^2K_Z{}^2} + \frac{C_T}{16\mu_b{}^3 l K_X{}^2K_Z{}^2}\left\{\frac{1}{2}\left(C_{l_p}C_{n_r} - C_{n_p}C_{l_r}\right) + 4\mu_b\left(K_X{}^2C_{n_\beta} - K_{XZ}C_{l_\beta}\right) + (z + l\sin\zeta)\left(C_{n_\beta}C_{l_r} - C_{l_\beta}C_{n_r}\right) + (x + l\cos\zeta)\left(C_{l_\beta}C_{n_p} - C_{n_\beta}C_{l_p}\right) + z\left[4\mu_b\left(K_Z{}^2C_W + K_{XZ}C_{Y_\beta}\right) + (z + l\sin\zeta)\left(4\mu_b C_{n_\beta} + C_{Y_\beta}C_{n_r}\right) - C_{Y_\beta}C_{n_p}(x + l\cos\zeta)\right] - x\left[4\mu_b\left(K_X{}^2C_{Y_\beta} + K_{XZ}C_W\right) + (z + l\sin\zeta)\left(4\mu_b C_{l_\beta} + C_{Y_\beta}C_{l_r}\right) - C_{Y_\beta}C_{l_p}(x + l\cos\zeta)\right]\right\}$$

$$\begin{aligned}
A_3 = {} & \frac{C_{Y_\beta}\left(C_{n_p}C_{l_r} - C_{n_r}C_{l_p}\right) + 4\mu_b\left(C_{l_\beta}C_{n_p} - C_{n_\beta}C_{l_p}\right) + 8\mu_b C_W\left(K_{XZ}C_{n_\beta} - K_Z{}^2C_{l_\beta}\right)}{32\mu_b{}^3K_X{}^2K_Z{}^2} + \\
& \frac{C_T}{8\mu_b{}^2 l K_X{}^2K_Z{}^2}\Bigg\{2(x + l\cos\zeta)\left(K_X{}^2C_{n_\beta} - K_{XZ}C_{l_\beta}\right) + \\
& 2(z + l\sin\zeta)\left(K_Z{}^2C_{l_\beta} - K_{XZ}C_{n_\beta}\right) + K_{XZ}\left(C_{n_p} + C_{l_r}\right) - K_X{}^2C_{n_r} - K_Z{}^2C_{l_p} + \\
& z\left[(x + l\cos\zeta)\left(C_{n_p} + 2K_{XZ}C_{Y_\beta}\right) - (z + l\sin\zeta)\left(C_{n_r} + 2K_Z{}^2C_{Y_\beta}\right)\right] + \\
& x\left[(z + l\sin\zeta)\left(C_{l_r} + 2K_{XZ}C_{Y_\beta}\right) - (x + l\cos\zeta)\left(C_{l_p} + 2K_X{}^2C_{Y_\beta}\right)\right]\Bigg\}
\end{aligned}$$

$$\begin{aligned}
A_4 = {} & \frac{1}{16\mu_b{}^2K_X{}^2K_Z{}^2}\Big[\left(C_{l_p}C_{n_r} - C_{n_p}C_{l_r}\right) - 2K_{XZ}C_{Y_\beta}\left(C_{n_p} + C_{l_r}\right) + \\
& 2K_Z{}^2C_{Y_\beta}C_{l_p} + 2K_X{}^2C_{Y_\beta}C_{n_r} + 8\mu_bK_X{}^2C_{n_\beta} - 8\mu_bK_{XZ}C_{l_\beta}\Big] + \\
& \frac{C_T}{2\mu_b l K_X{}^2K_Z{}^2}\Bigg\{K_X{}^2K_Z{}^2 + z\left[K_Z{}^2(z + l\sin\zeta) - K_{XZ}(x + l\cos\zeta)\right] + \\
& x\left[K_X{}^2(x + l\cos\zeta) - K_{XZ}(z + l\sin\zeta)\right]\Bigg\}
\end{aligned}$$

$$A_5 = \frac{1}{4\mu_bK_X{}^2K_Z{}^2}\left[K_{XZ}\left(C_{n_p} + C_{l_r}\right) - K_Z{}^2C_{l_p} - K_X{}^2C_{n_r} - 2K_X{}^2K_Z{}^2C_{Y_\beta}\right]$$

REFERENCES

1. Bryant, L. W., Brown, W. S., and Sweeting, N. E.: Collected Researches on the Stability of Kites and Towed Gliders. R. & M. No. 2303, British A.R.C., 1942.

2. Maggin, Bernard, and Shanks, Robert E.: Experimental Determination of the Lateral Stability of a Glider Towed by a Single Towline and Correlation With an Approximate Theory. NACA RM L8H23, 1948.

3. Schade, Robert O., and Hassell, James L., Jr.: The Effects on Dynamic Lateral Stability and Control of Large Artificial Variations in the Rotary Stability Derivatives. NACA TN 2781, 1952.

4. Mitchell, K.: Estimation of the Effect of a Parameter Change on the Roots of Stability Equations. Aeronautical Quarterly, vol. I, pt. I, May 1949, pp. 39-58.

TABLE I.- MASS AND AERODYNAMIC PARAMETERS OF HIGH-SPEED FIGHTER

USED IN EXAMPLE AND TOWLINE PARAMETERS OF BASIC CASE

Altitude, ft	50,000
W/S, lb/sq ft	52.5
S, sq ft	476
b, ft	38.4
ρ, slugs/cu ft	0.000361
V, ft/sec	1459.5
γ, deg	0
C_W	0.138
C_D	0.034
μ_b	117.66
${K_X}^2$	0.0125
${K_Z}^2$	0.1376
K_{XZ}	0.004886
α, deg	2.4
ϵ, deg	0
η, deg	2.4
C_{l_p}, per radian	-0.355
C_{l_r}, per radian	0.0228
C_{n_p}, per radian	-0.0514
C_{n_r}, per radian	-0.670
C_{Y_β}, per radian	-0.488
C_{n_β}, per radian	0.241
C_{l_β}, per radian	-0.0373
Towline parameters of basic case:	
z, spans	0.022
x, spans	0.52
l, spans	26.0
ζ, deg	0
C_T	0.034

NACA

TABLE II.- CHARACTERISTIC MODES

Row	Type of system	Towline oscillation		Spiral mode	Damping in roll	Dutch roll	
		$T_{1/2}$, sec	P, sec	$T_{1/2}$, sec	$T_{1/2}$, sec	$T_{1/2}$, sec	P, sec
1	Airplane alone	--------	--------	142	0.307	2.80	1.87
2	Airplane with towline (basic)	-5.58	24.0	2.68	.306	2.86	1.81
3	l = 2.6 spans (100 ft)	-2.56	11.4	1.20	.310	2.84	1.80
4	l = 13 spans (500 ft)	-4.35	19.3	2.08	.307	2.86	1.80
5	l = 130 spans (5,000 ft)	-11.1	37.1	5.19	.306	2.86	1.81
6	$l = \infty$	184	51.5	--------	.304	2.70	1.80
7	l = 26 spans; z = -0.0804 span	116	52.1	567	.307	2.84	1.80
8	z = 3.0 spans	15.3	11.3	{ $T_{1/2}$ = 0.582 sec, P = 3.08 sec }		4.84	1.95
9	Connection at center of gravity	134	70.9	--------	.307	2.88	1.87
10	Side-force autopilot; K' = -1.92	-16.2	27.4	1.73	.305	2.85	1.81
11	Side-force autopilot; K' = -1.92; z = -0.0805 span	4.46	50.1	--------	.305	2.86	1.81
12	Rudder-type autopilot; K' = -1.92	5.32	8.07	21.0	.283	4.28	1.82
13	Roll autopilot; $\Delta T_{l\phi}$ = -0.015	110	42.0	{ $T_{1/2}$ = 0.648 sec, P = 2.64 sec }		2.28	1.78
14	Roll autopilot; $\Delta T_{l\phi}$ = -0.100	126	47.1	{ $T_{1/2}$ = 0.614 sec, P = 0.900 sec }		2.82	1.86
15	Acceleration autopilot; K' = -1.92 sec	-810	44.7	1.28	.367	3.98	1.69

NACA

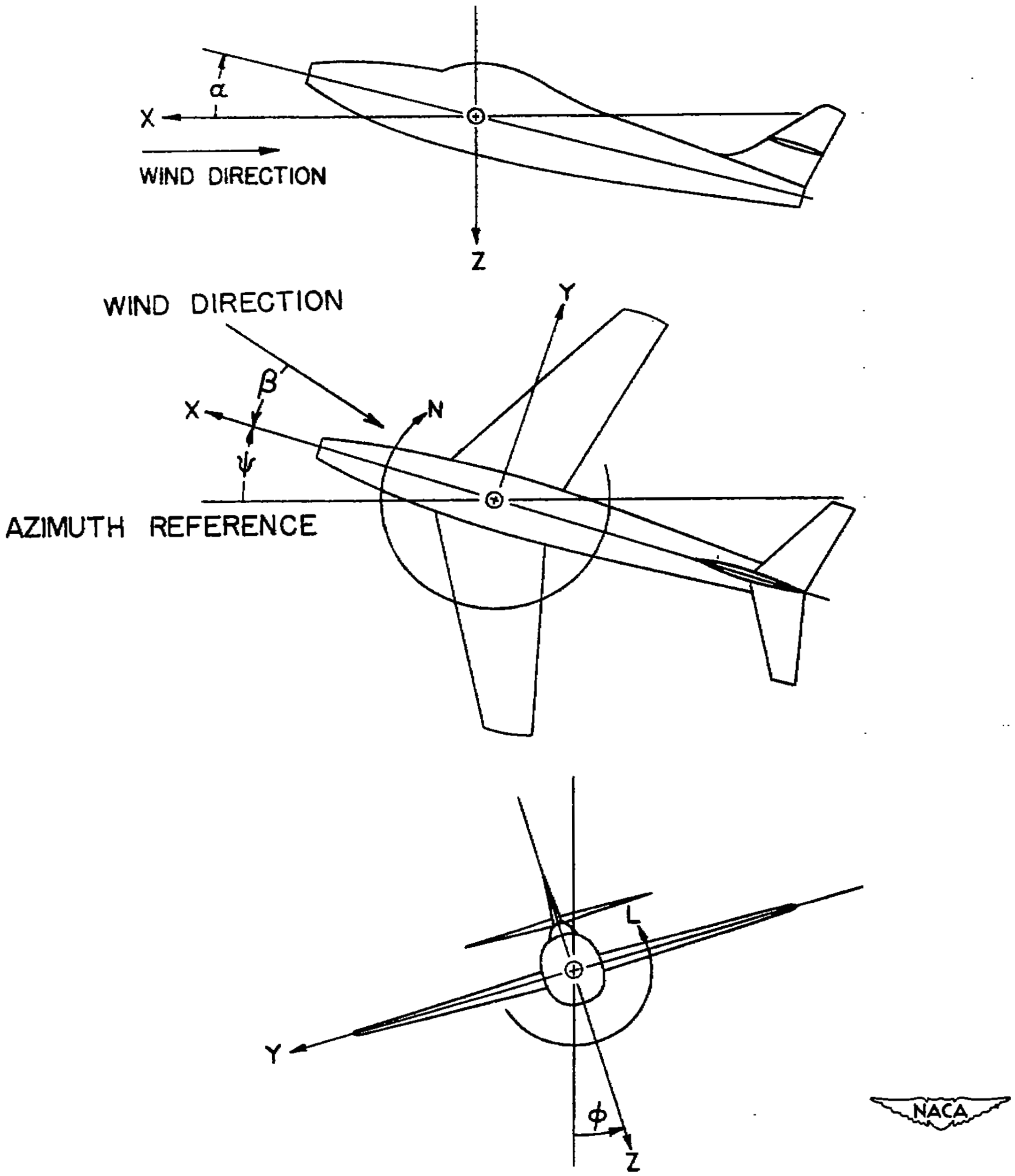

Figure 1.- The stability system of axes. Arrows indicate positive directions of moments, forces, and angles. This system of axes is defined as an orthogonal system having the origin at the center of gravity and the Z-axis in the plane of symmetry and perpendicular to the relative wind, the X-axis in the plane of symmetry and perpendicular to the Z-axis, and the Y-axis perpendicular to the plane of symmetry.

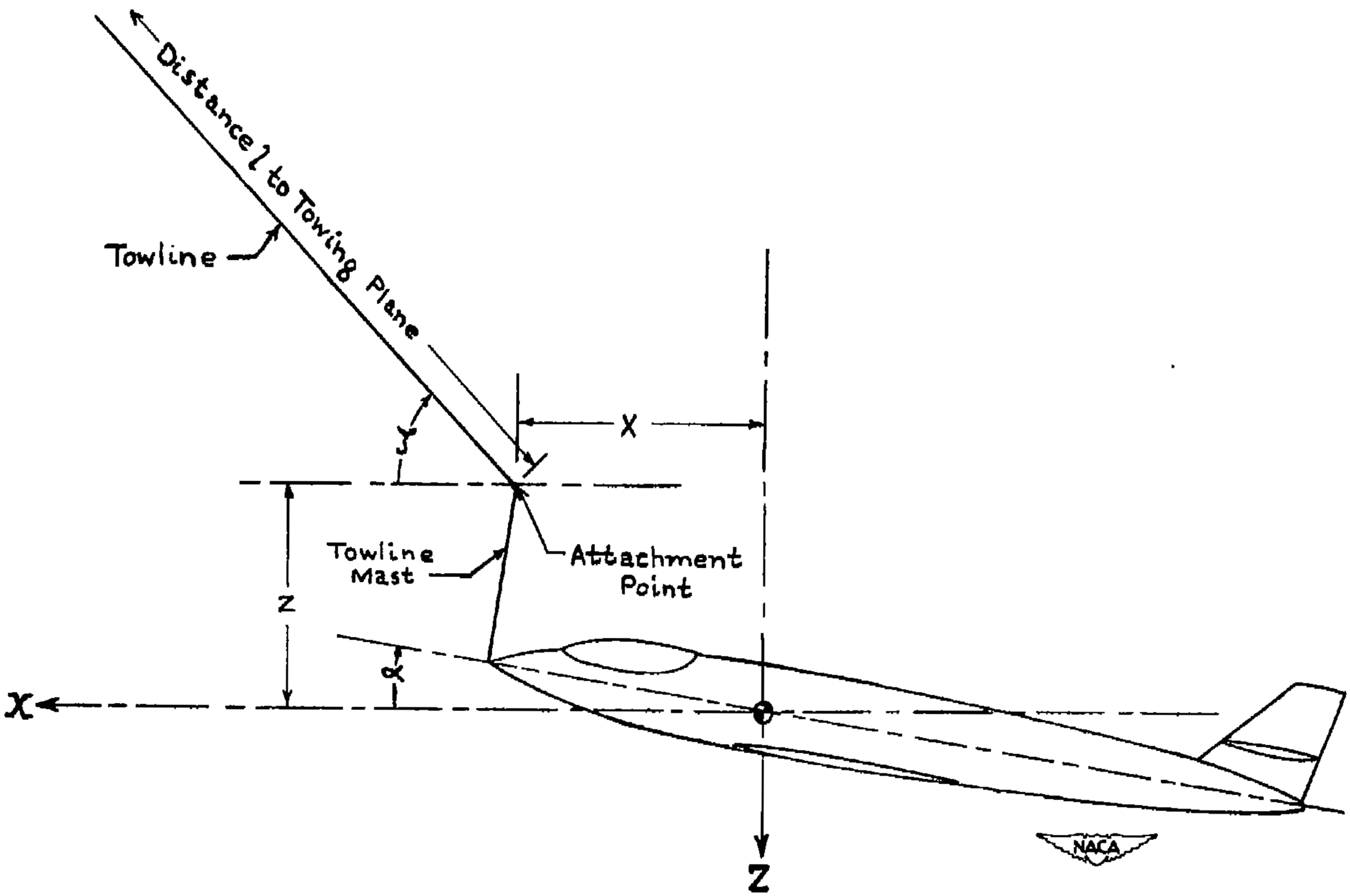

Figure 2.- High-speed fighter airplane with towline attached.

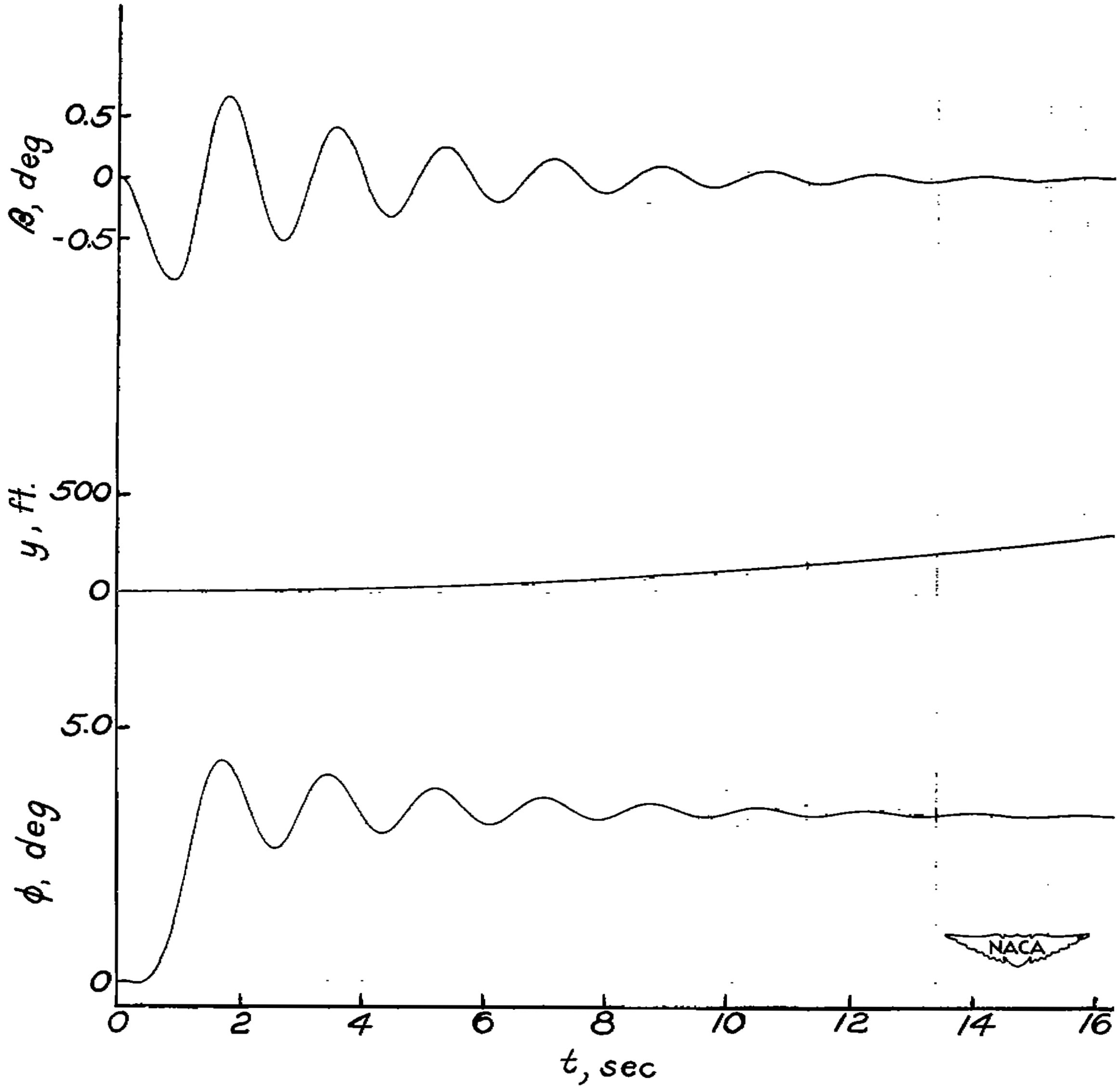

(a) Rudder kick, 2° for 1 second.

Figure 3.- Motions of free airplane subsequent to three types of disturbance.

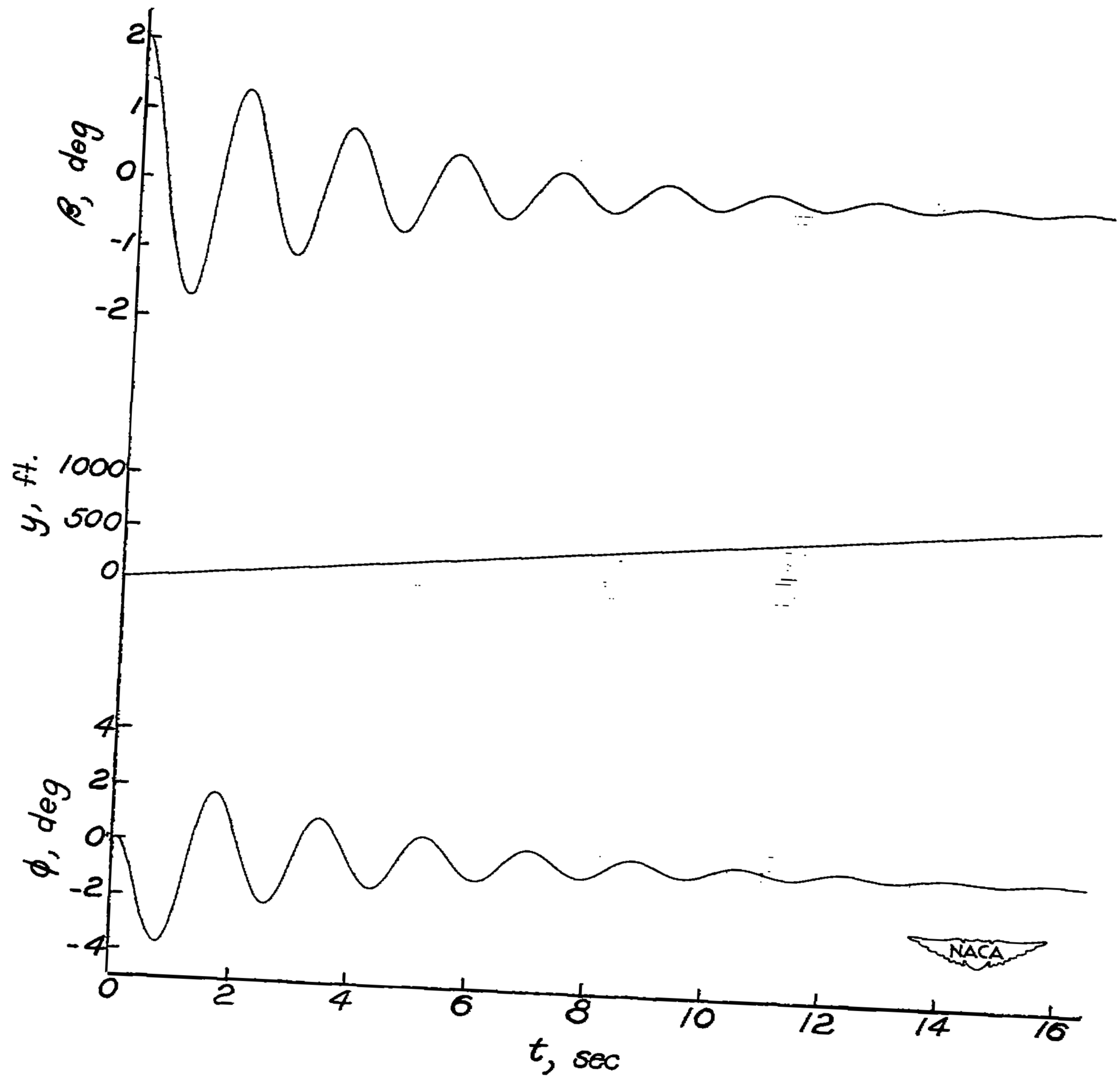

(b) $\beta_o = 2^\circ$.

Figure 3.- Continued.

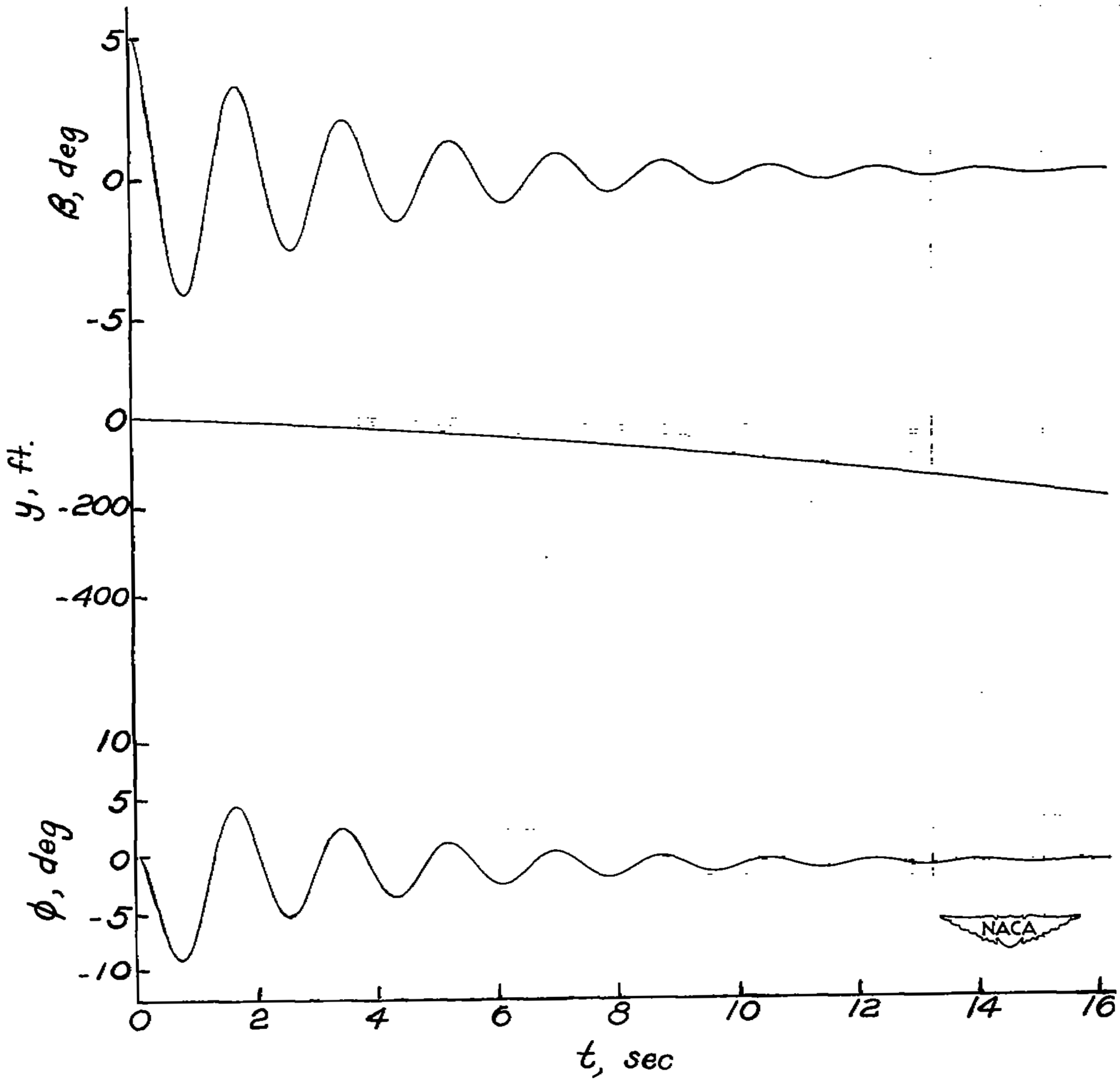

(c) $\psi_o = -5^\circ$; $\beta_o = 5^\circ$.

Figure 3.- Concluded.

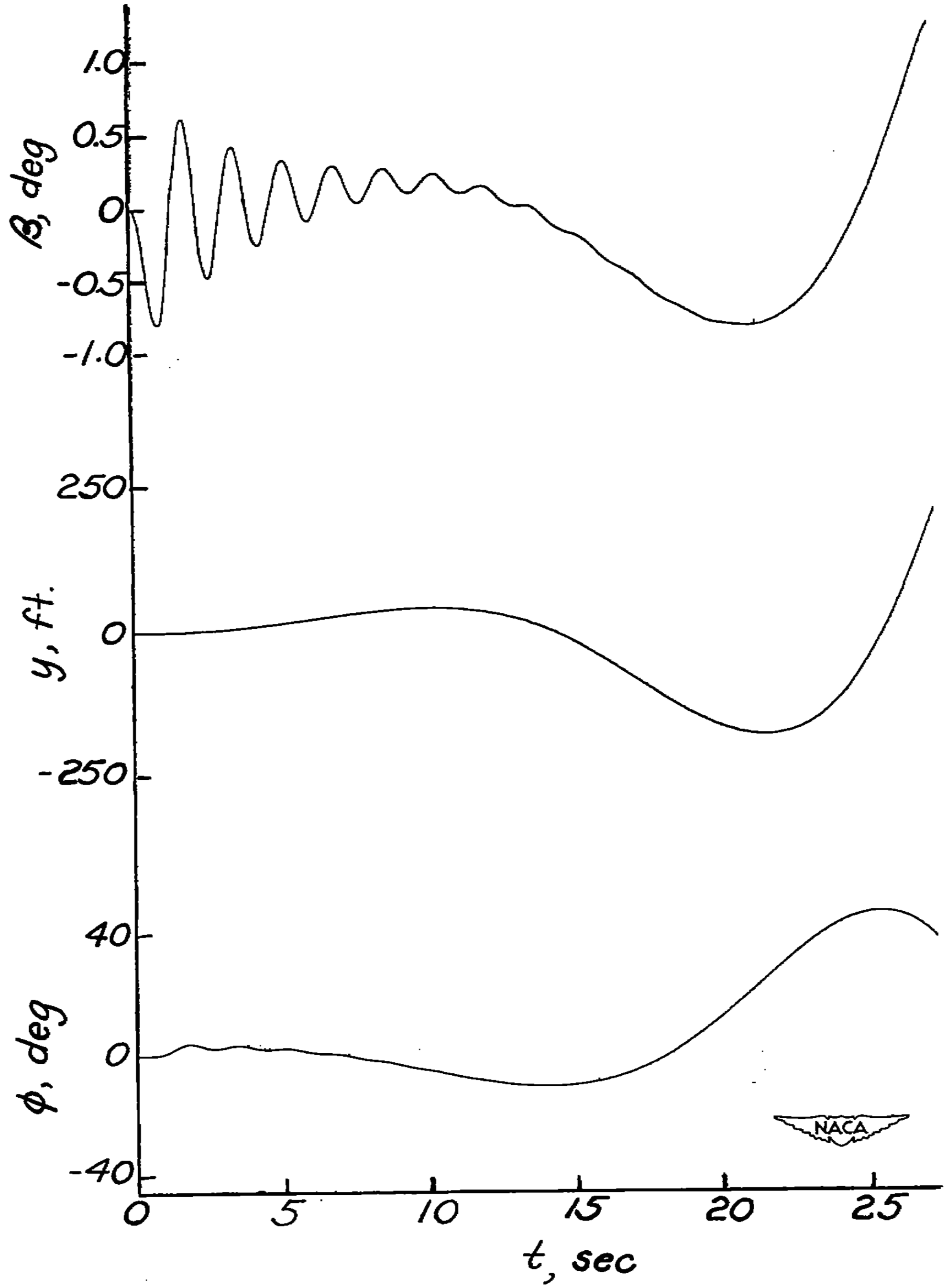

(a) Rudder kick, 2° for 1 second.

Figure 4.- Motions of airplane with nose attachment of towline (basic case) subsequent to three types of disturbance.

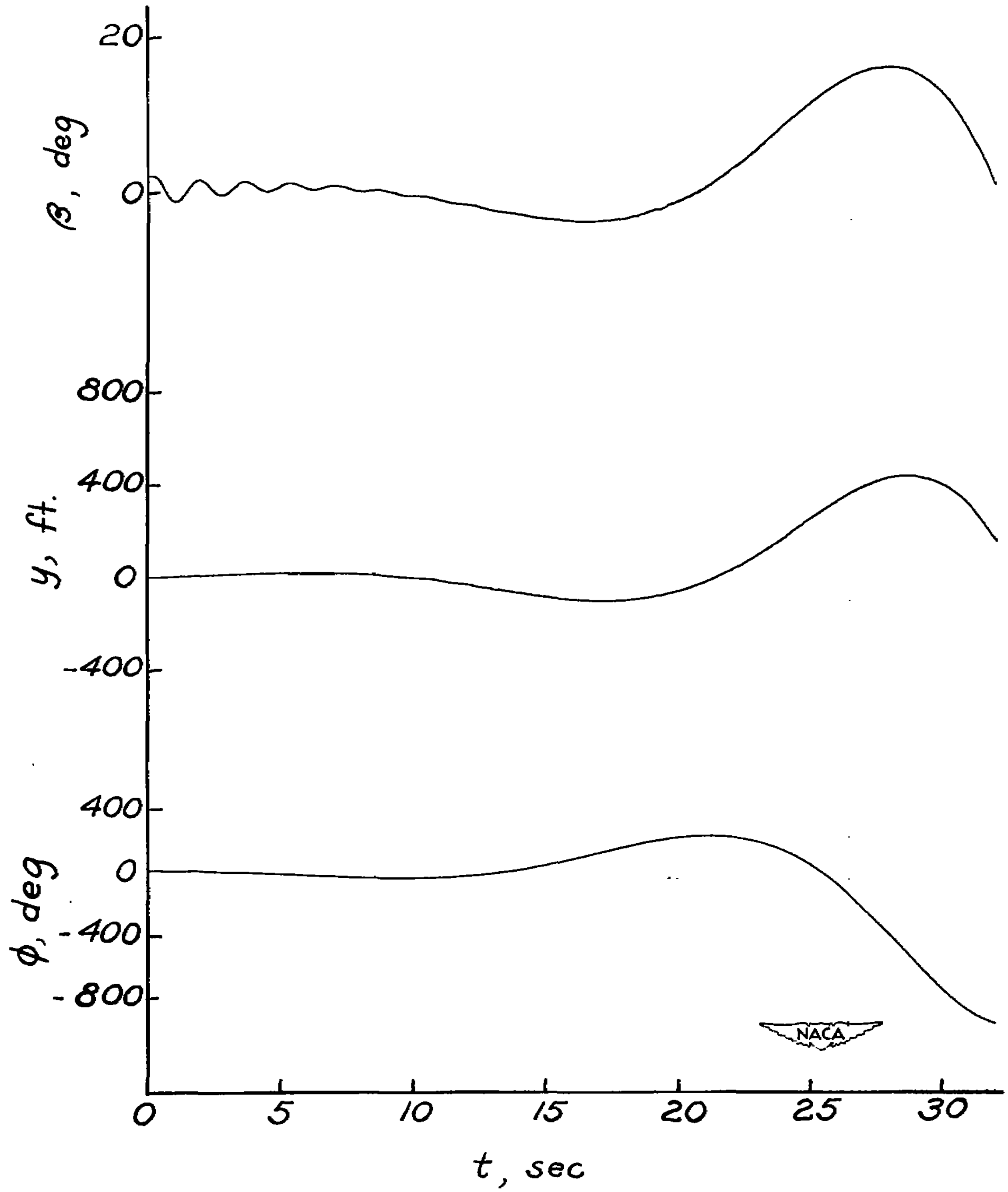

(b) $\beta_o = 2^\circ$.

Figure 4.- Continued.

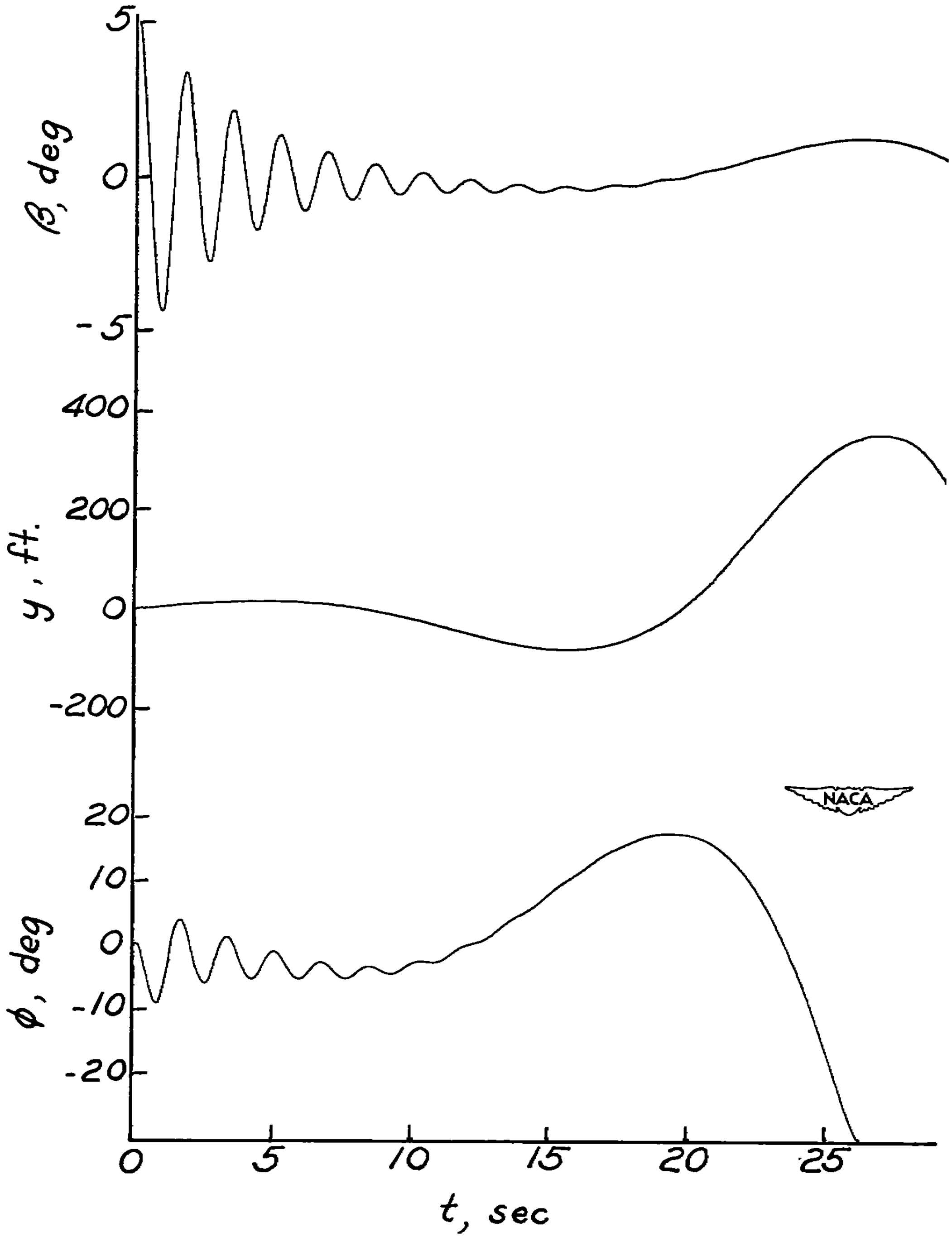

(c) $\psi_o = -5^\circ$; $\beta_o = 5^\circ$.

Figure 4.- Concluded.

[redacted]

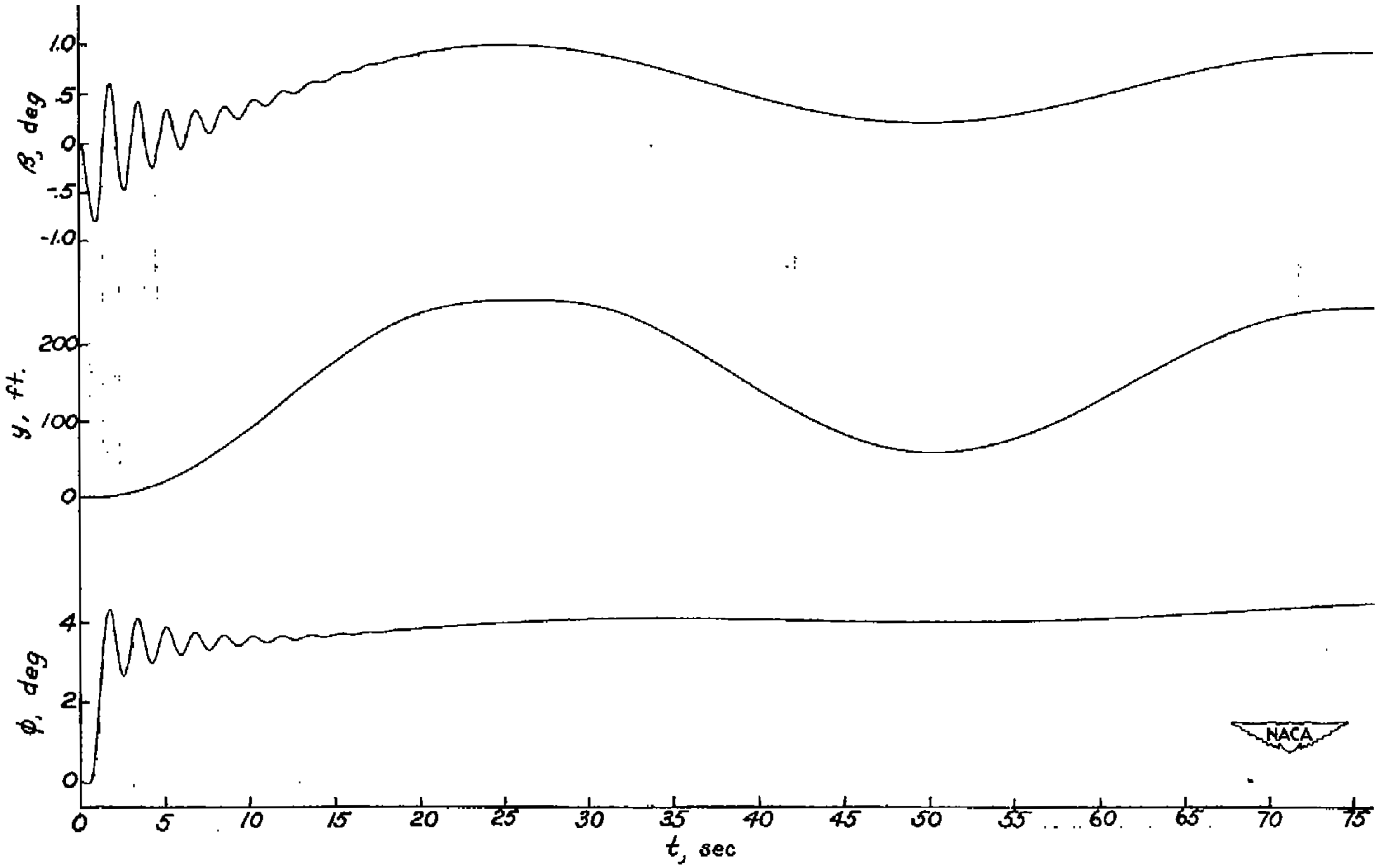

(a) Rudder kick, 2° for 1 second.

Figure 5.- Motions of airplane with towline attached to a short mast below the nose subsequent to two types of disturbance. z = -0.0804 span.

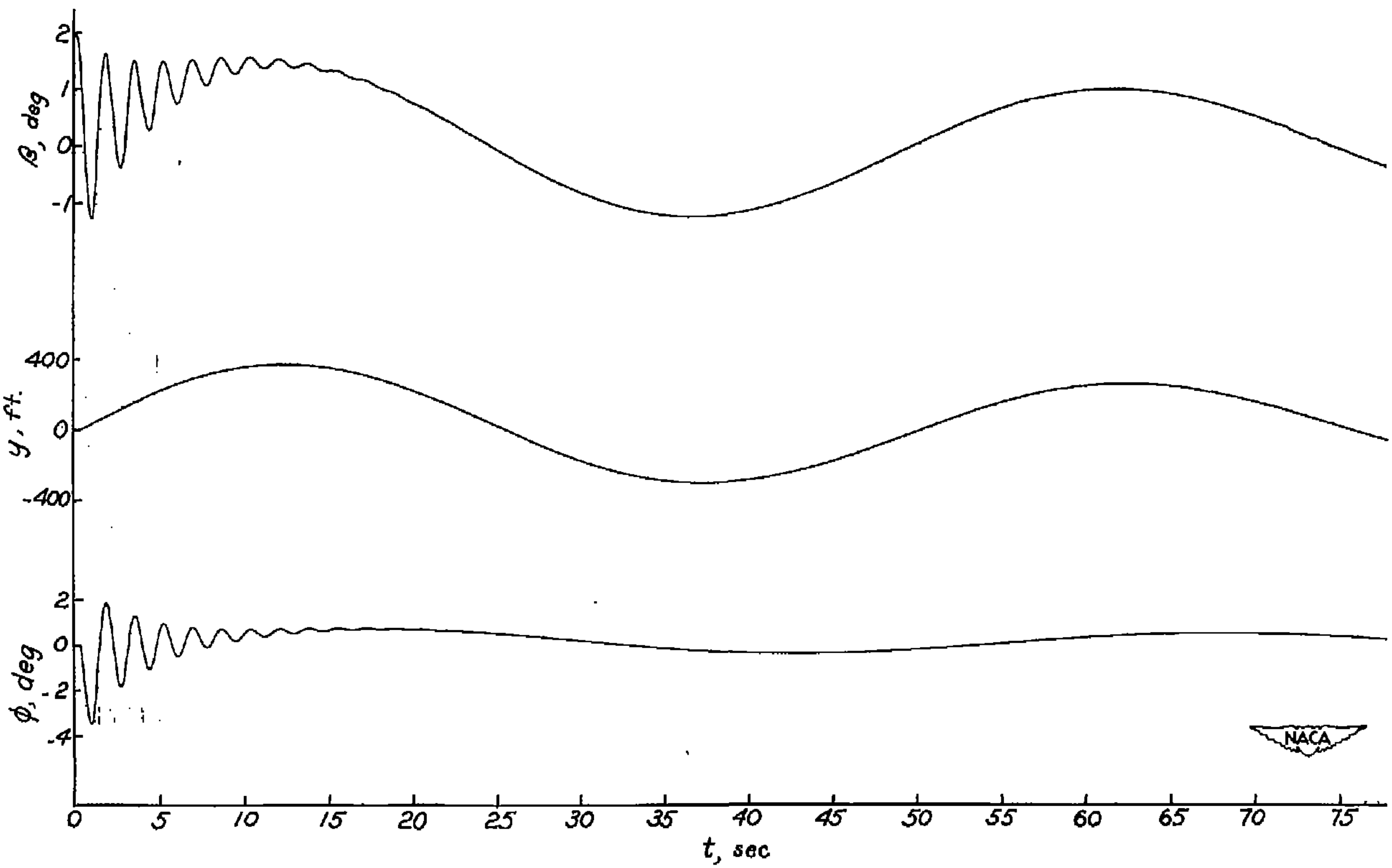

(b) $\beta_o = 2^\circ$.

Figure 5.- Concluded.

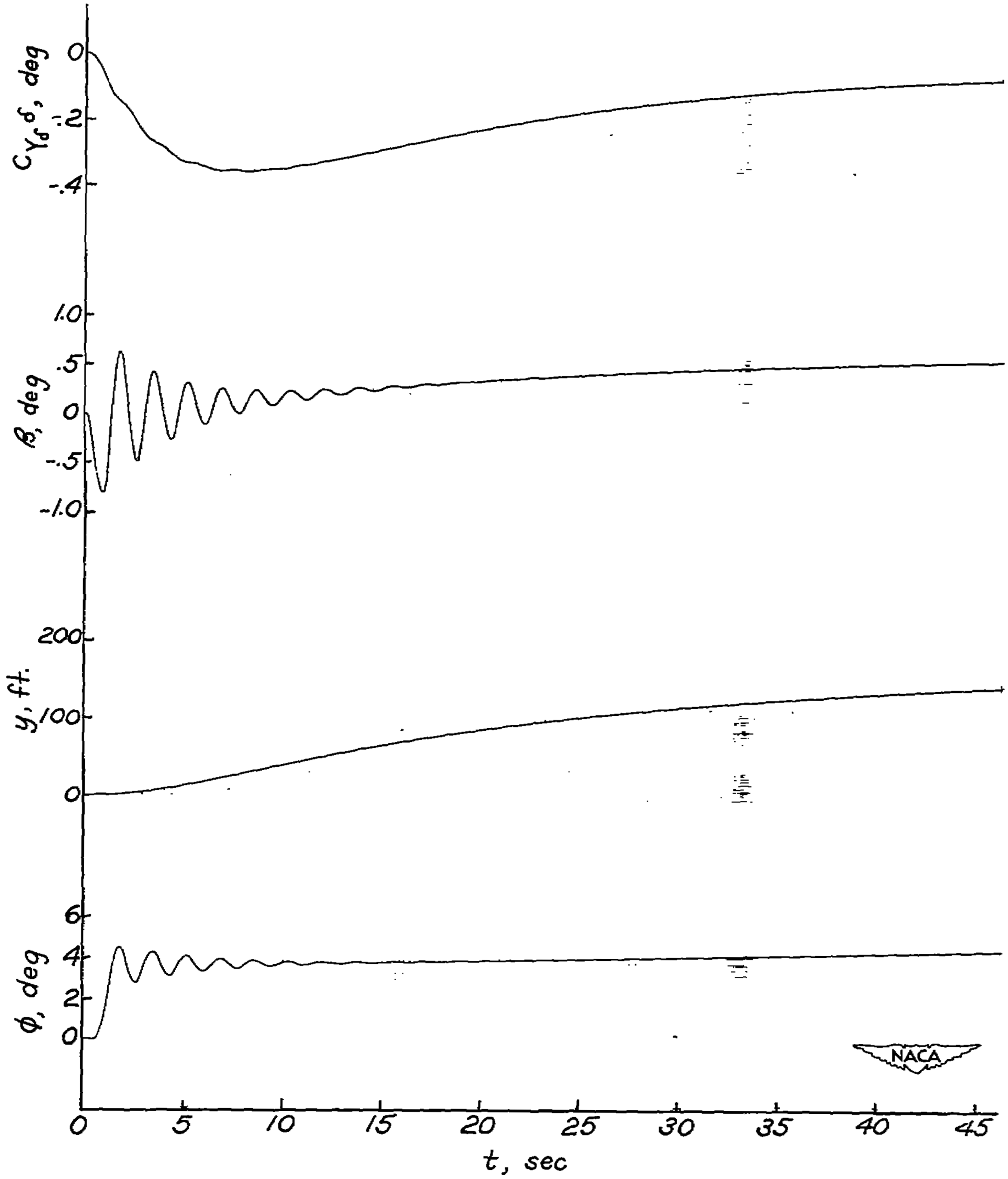

(a) Rudder kick, 2° for 1 second.

Figure 6.- Motions of airplane with side-force autopilot subsequent to two types of disturbance. K' = -1.92; z = -0.0804 span.

[redacted]

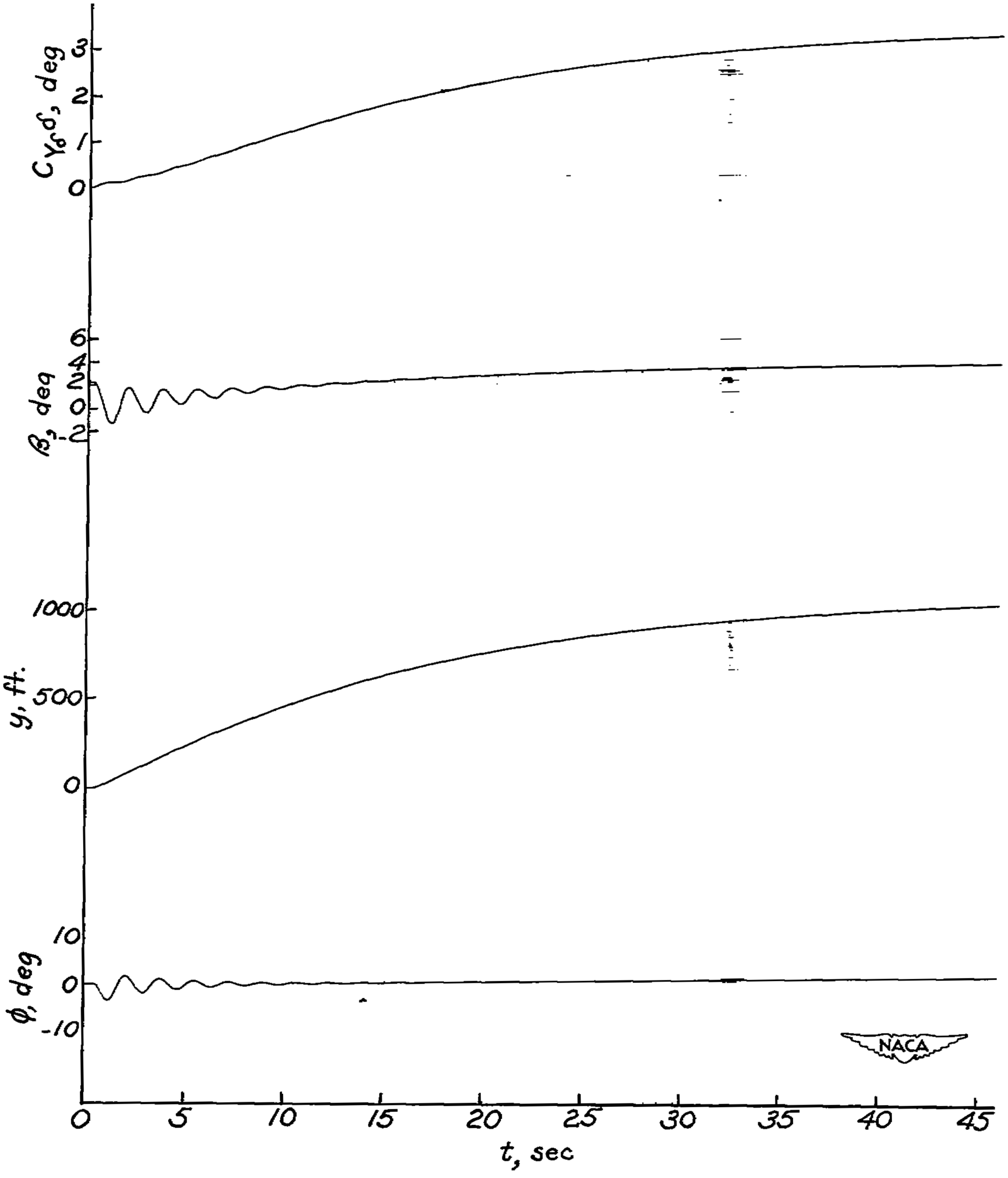

(b) $\beta_o = 2^\circ$.

Figure 6.- Concluded.

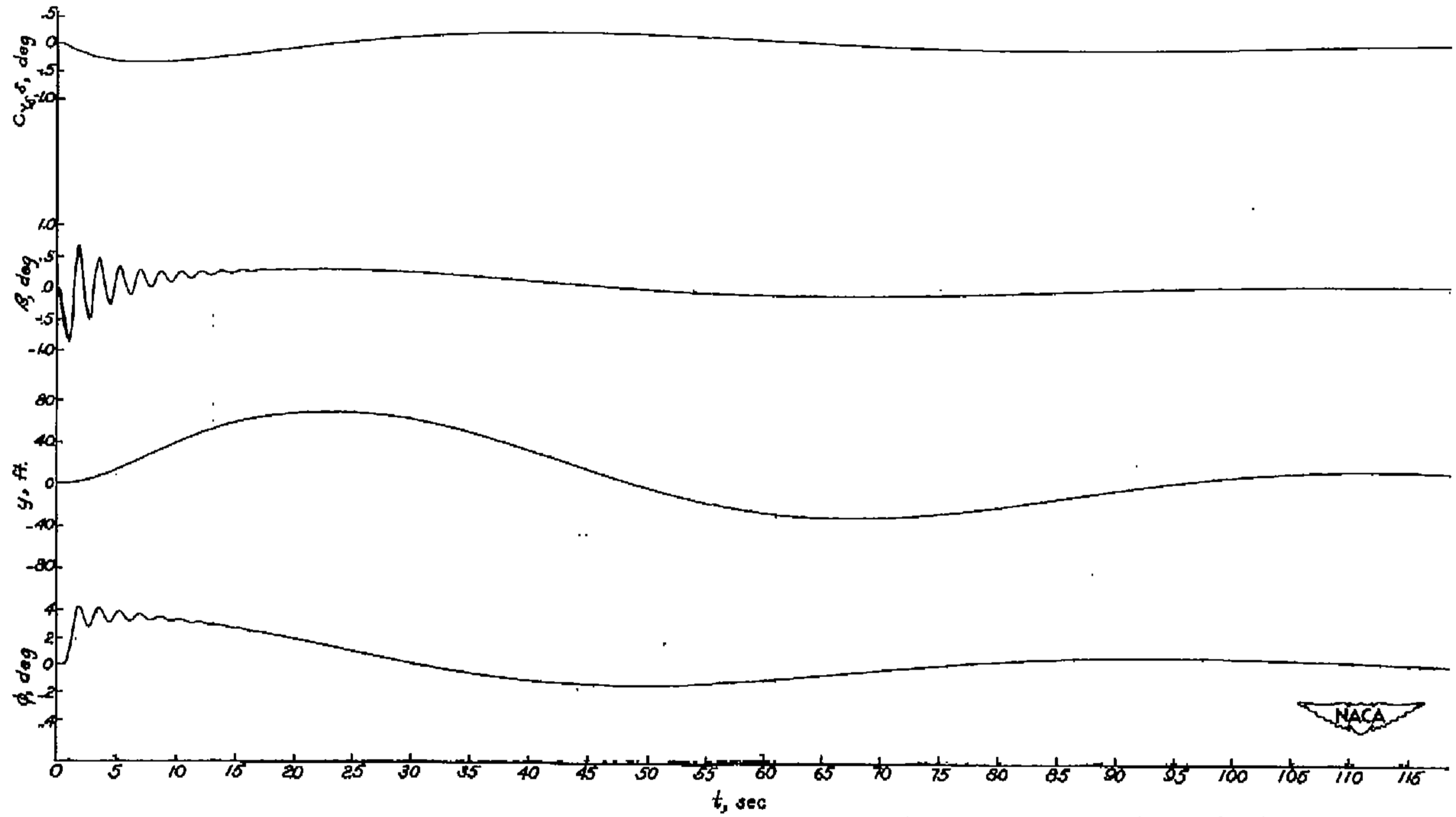

Figure 7.- Motion of airplane with side-force autopilot subsequent to rudder kick. K' = -1.92; z = -0.0740 span.

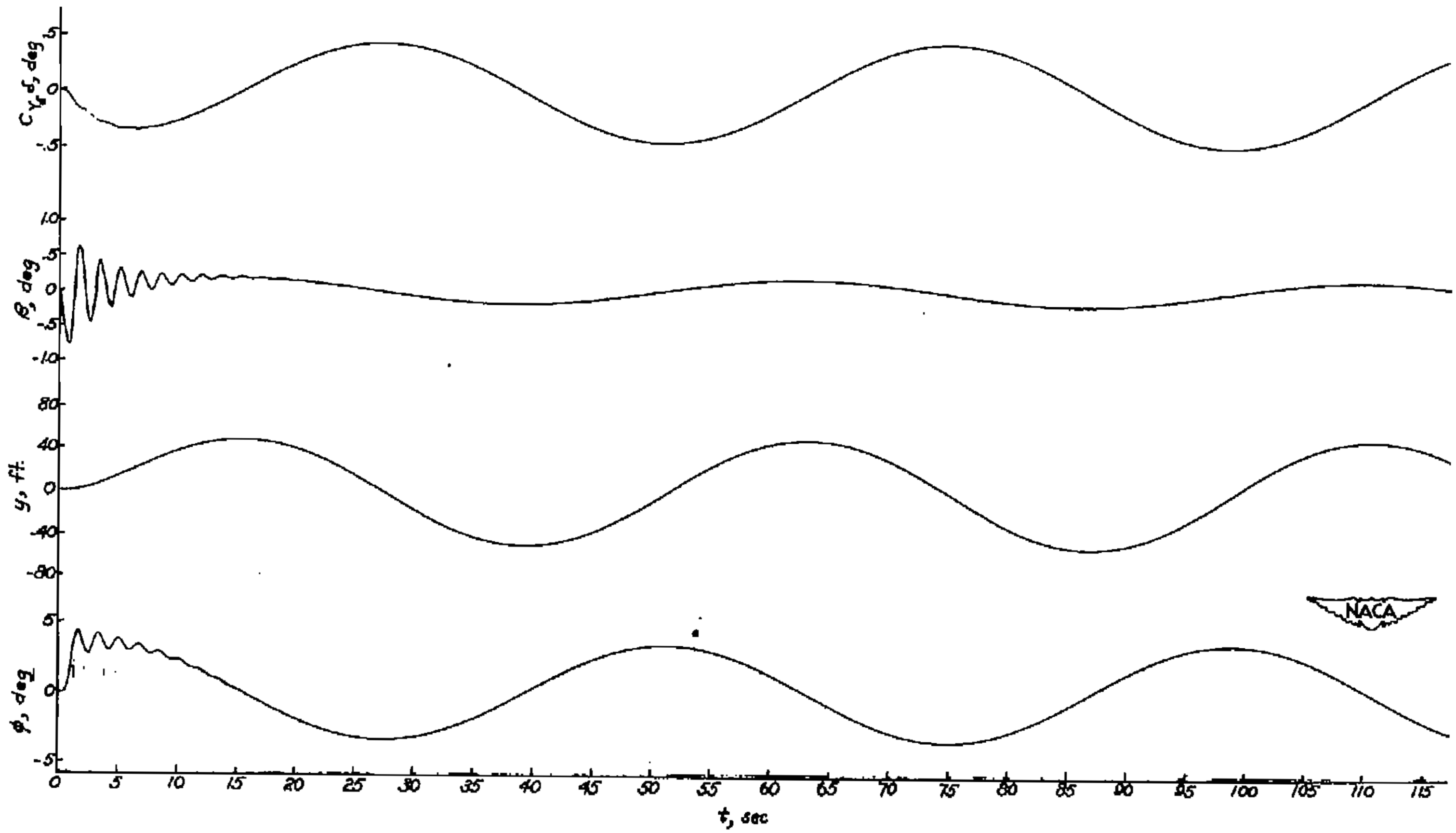

Figure 8.- Motion of airplane with side-force autopilot subsequent to rudder kick. K' = -1.92; z = -0.0544 span.

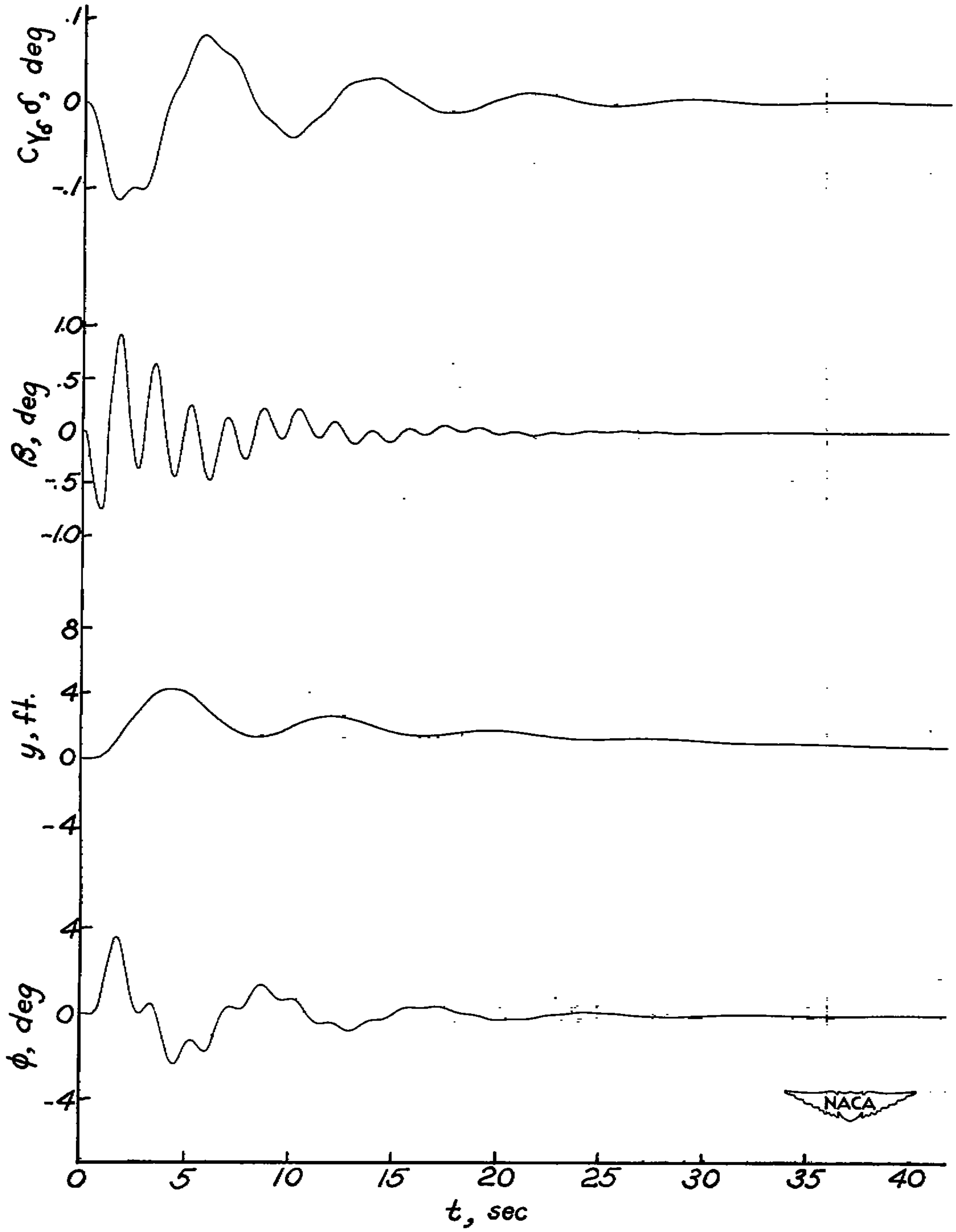

Figure 9.- Motion of airplane with automatically controlled rudder-type auxiliary control surface at the nose. K' = -1.92; z = 0.022 span; initial rudder kick.

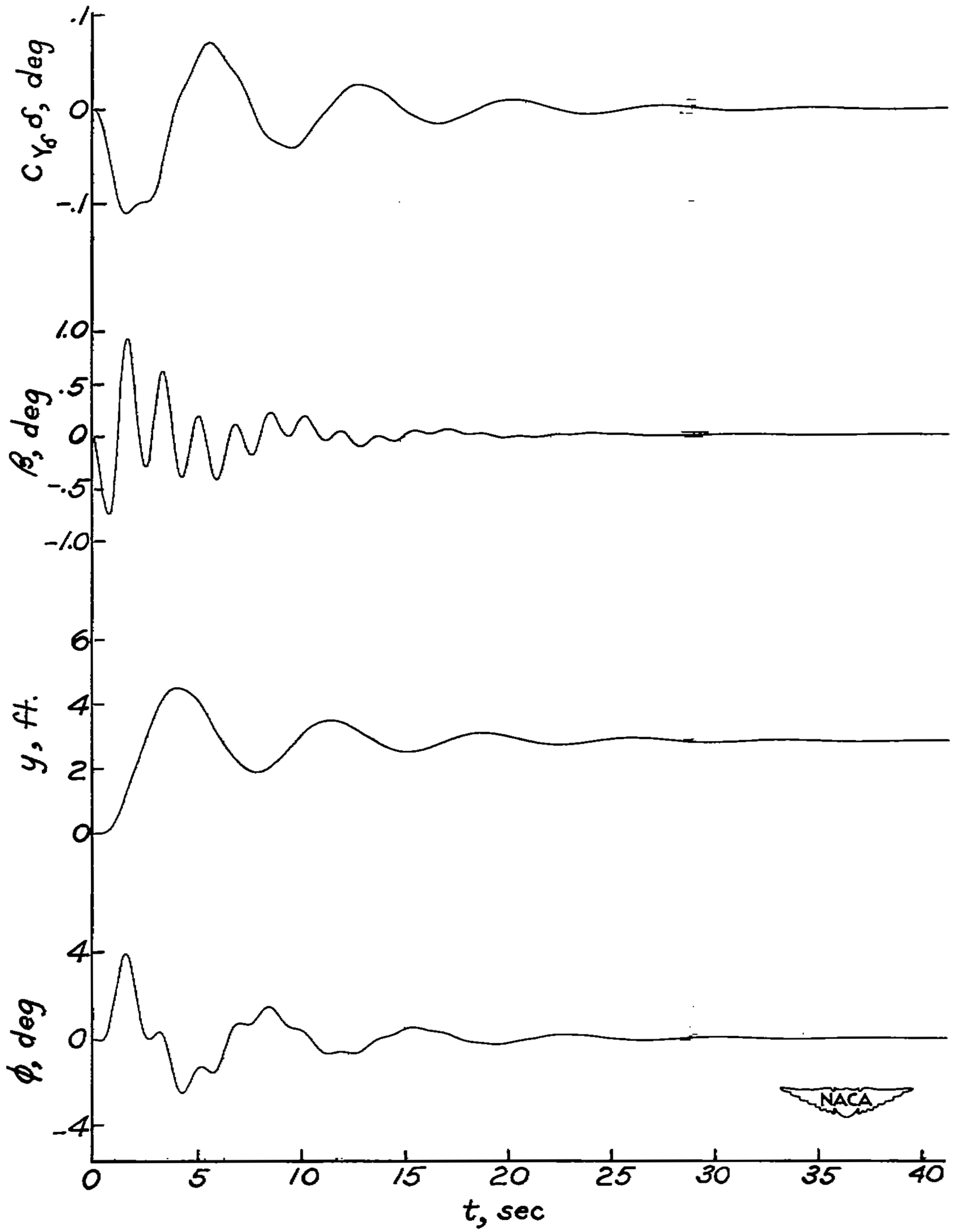

Figure 10.- Motion of airplane with automatically controlled rudder-type auxiliary control surface at the nose. K' = -1.92; z = -0.0804 span; initial rudder kick.

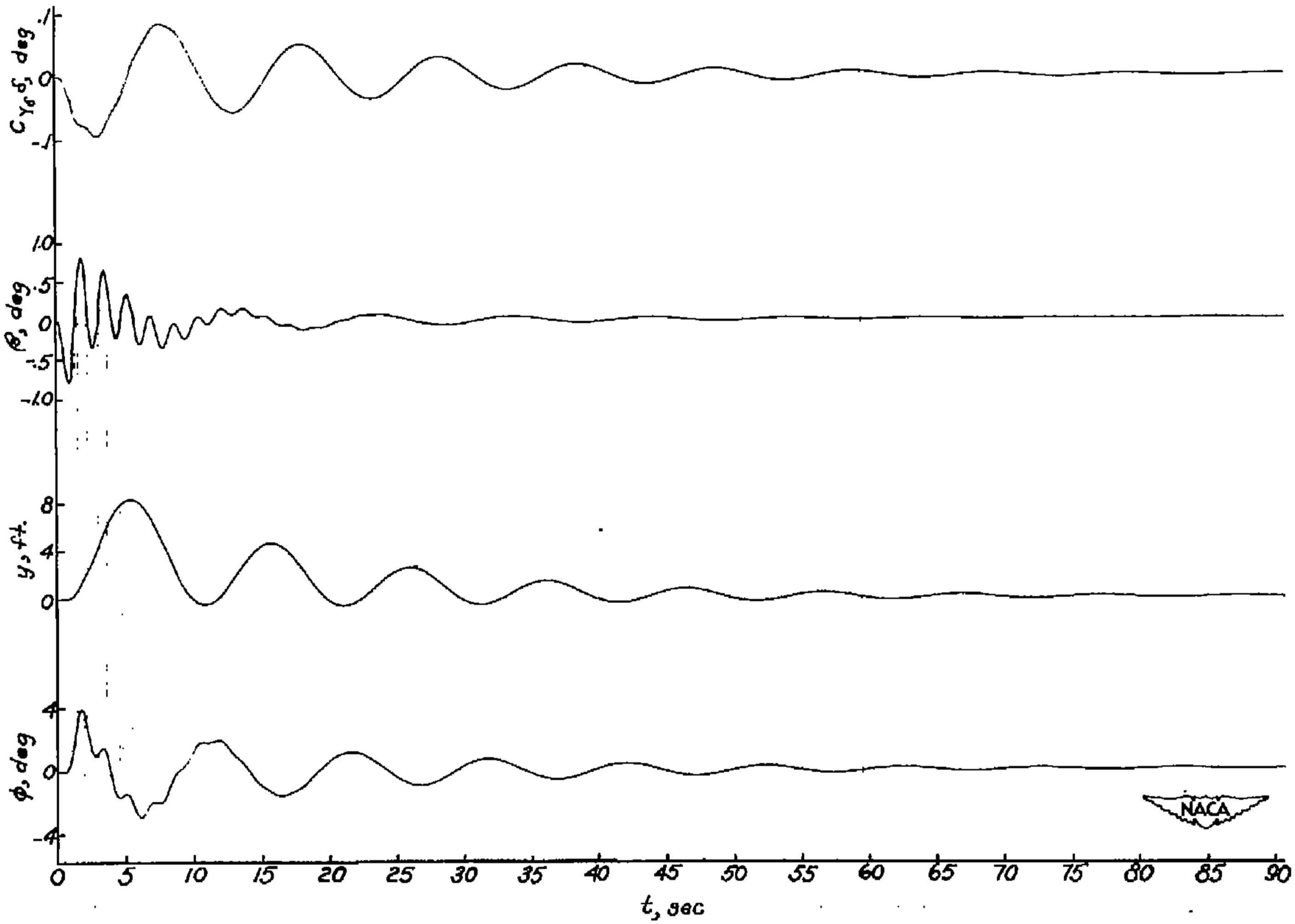

Figure 11.- Motion of airplane with automatically controlled rudder-type control surface at the nose. K' = -1.00; z = 0.022 span; initial rudder kick.

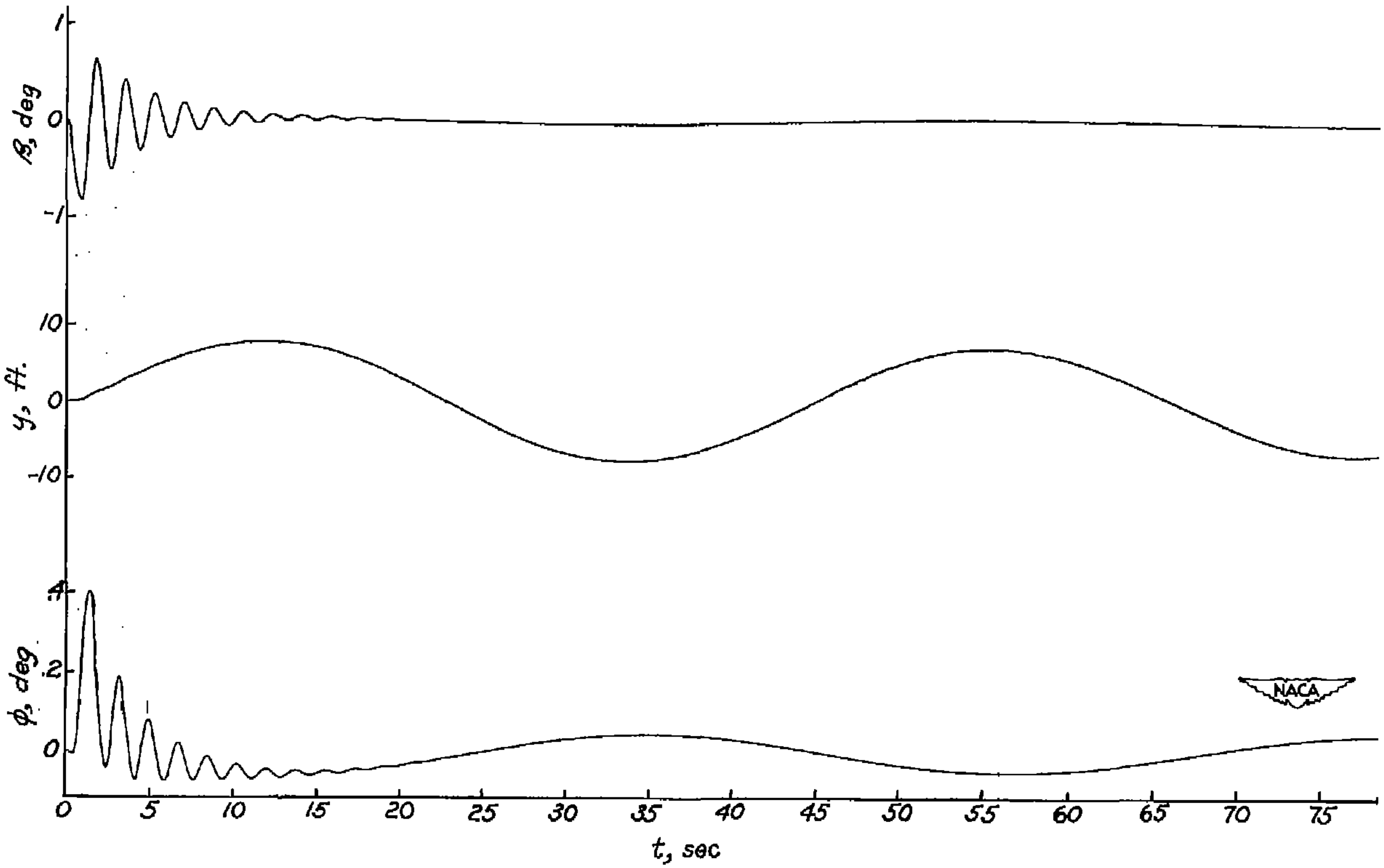

Figure 12.- Motion of airplane with aileron-type automatic control. $\Delta T_{l\phi} = -0.025$; z = 0.022 span; initial rudder kick.

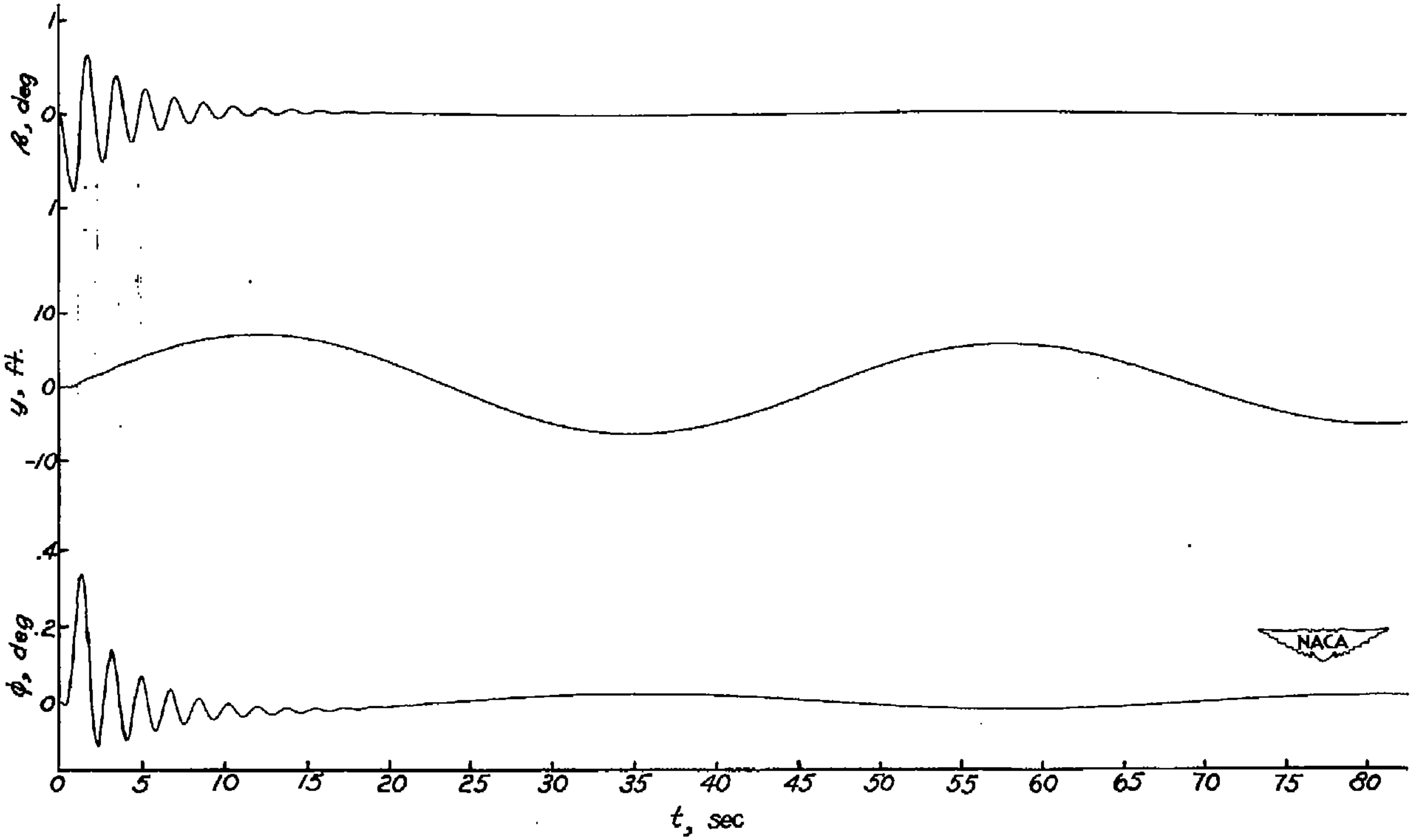

Figure 13.- Motion of airplane with aileron-type automatic control. $\Delta T_{l_\phi} = -0.050$; z = 0.022 span; initial rudder kick.